The extreme universe in messengers: from cosmic accelerators to beyond the standard model

Interpreting spectrum and composition of cosmic ray knees

Bing Theodore Zhang

Institute of High Energy Physics, CAS, China

Trieste, 2026/09/08

The spectrum of cosmic rays

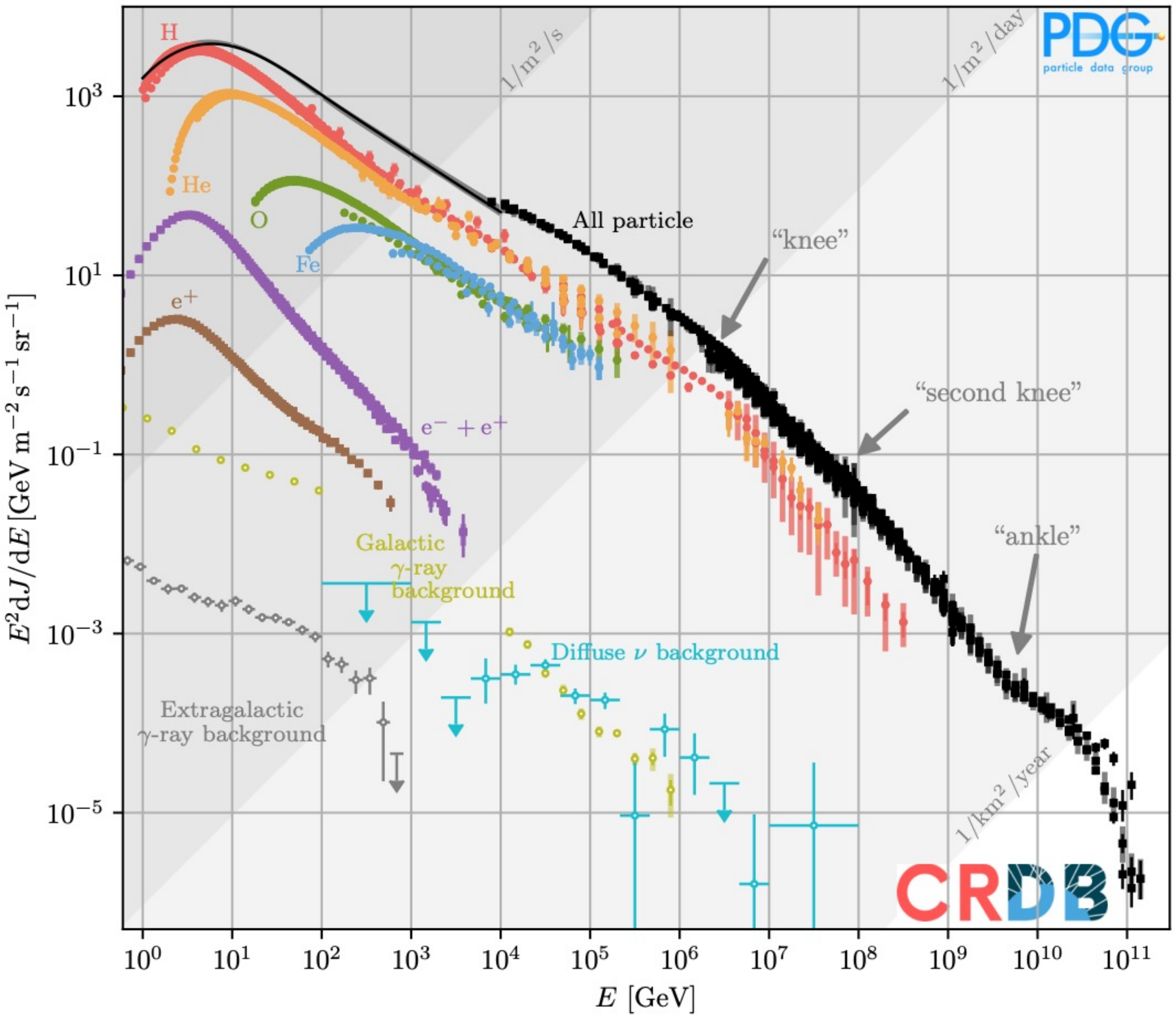

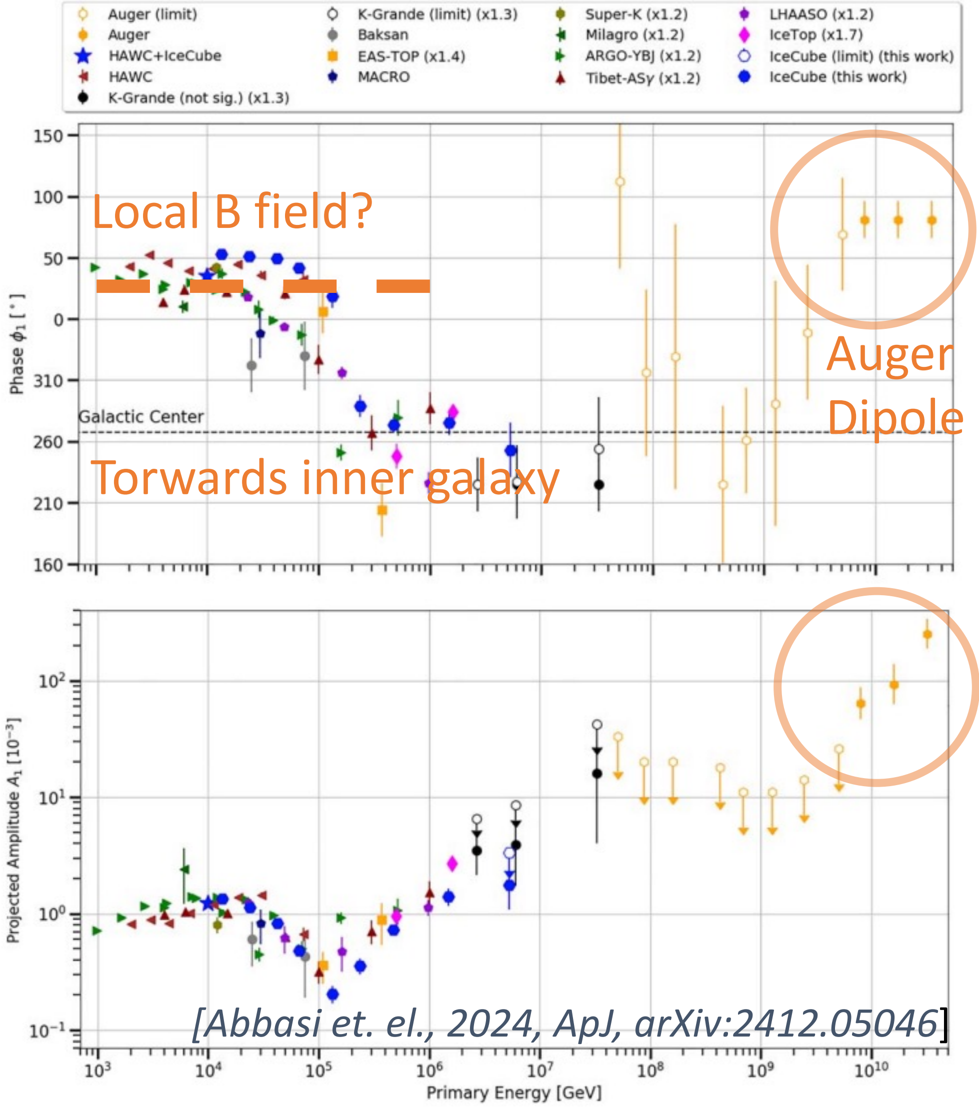

[Abbasi et. el., 2024, ApJ, arXiv:2412.05046]

Structures on the Galactic CR all-particle spectrum

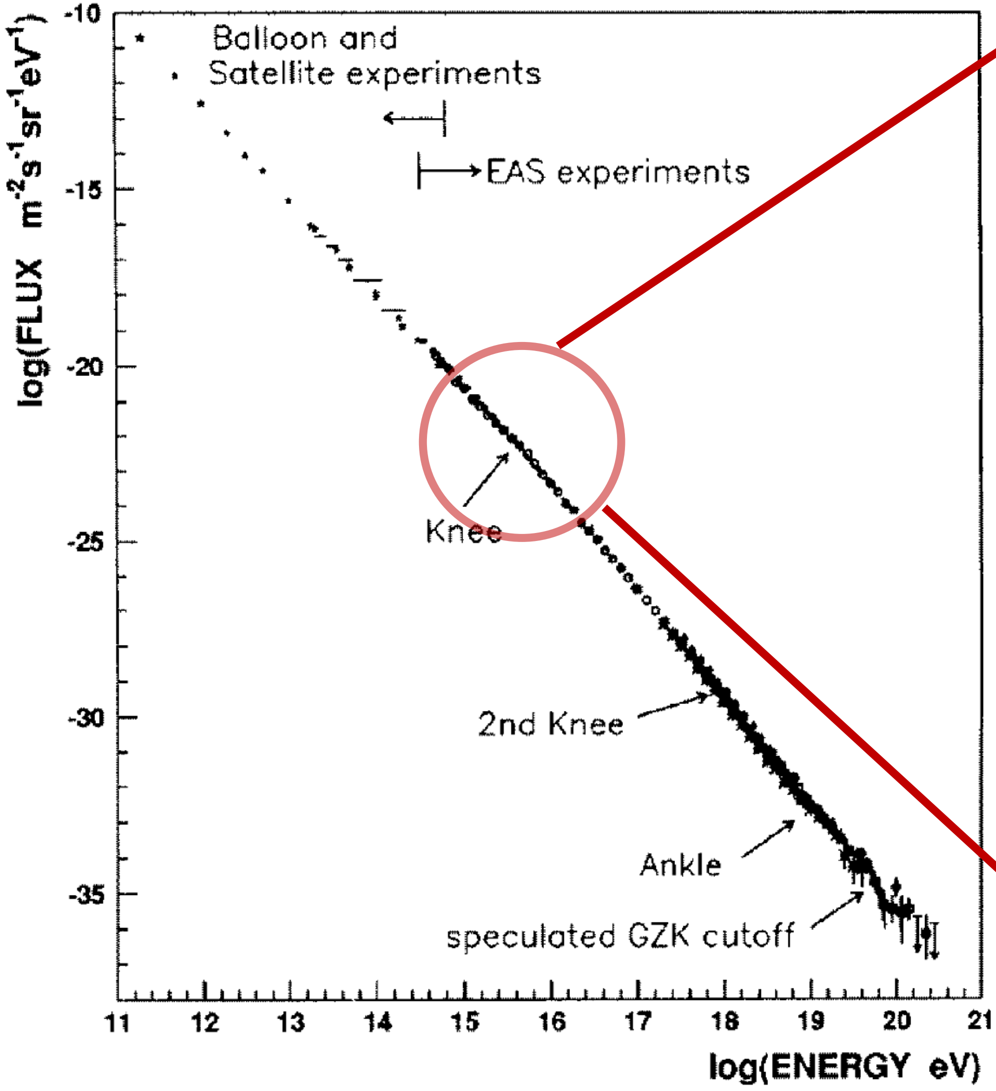

[*M. Nagano, A.A. Watson, Rev. Mod. Phys. 72 (2000) 689*]

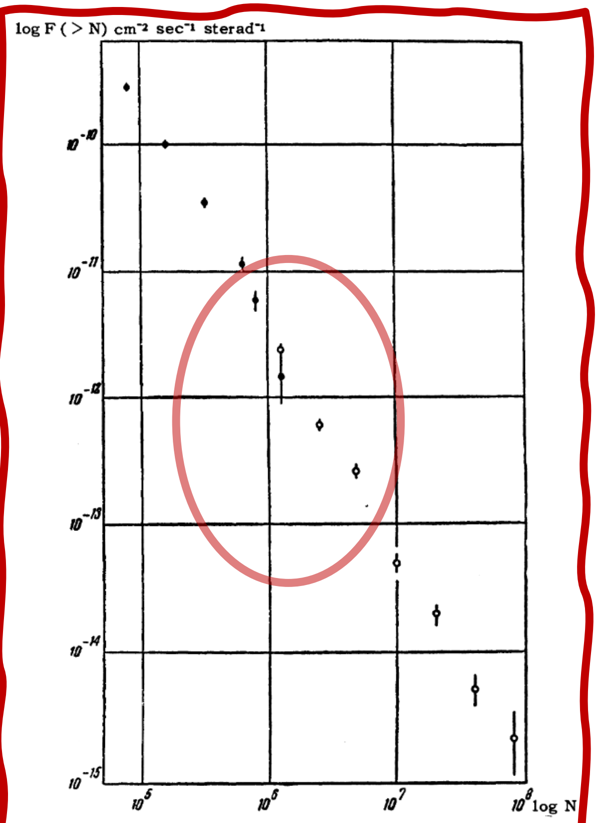

FIG. 2. Integral size spectrum of EAS. ● – measurements of the present experiment, ○ – measurements of reference 7.

[*Kulikov & Khristiansen, JETP, 55, 8, 1958*]

The data indicate with a high probability that a change in the character of the spectrum may occur in the investigated region $N = 8 \times 10^4$ to 1.5×10^6. In the region $N = 8 \times 10^4$ to 8×10^5 the integral spectrum can be approximated by a power law with an exponent $\kappa = 1.5 \pm 0.1$. For $N > 8 \times 10^5$ the spectrum is steeper. For a quantitative deter-

The knee is discoveried nearly seven decades ago, it has been established as a pronounced steepening of the all-particle CR spectrum at an energy of a few PeV

…while the origin is still a standard puzzle…

Origin of the CR knee

- Limitation of maximum acceleration energy

  [e.g., *Hillas 2005]*

  - Supernova remnants (SNRs) are widely belived to account for CRs at least up to the knee

- Propagation effects

  Changes on diffusion coefficient

  [e.g., *Syrovatsky (1971), Ptuskin (1992), Giacinti (2014,2015)]*

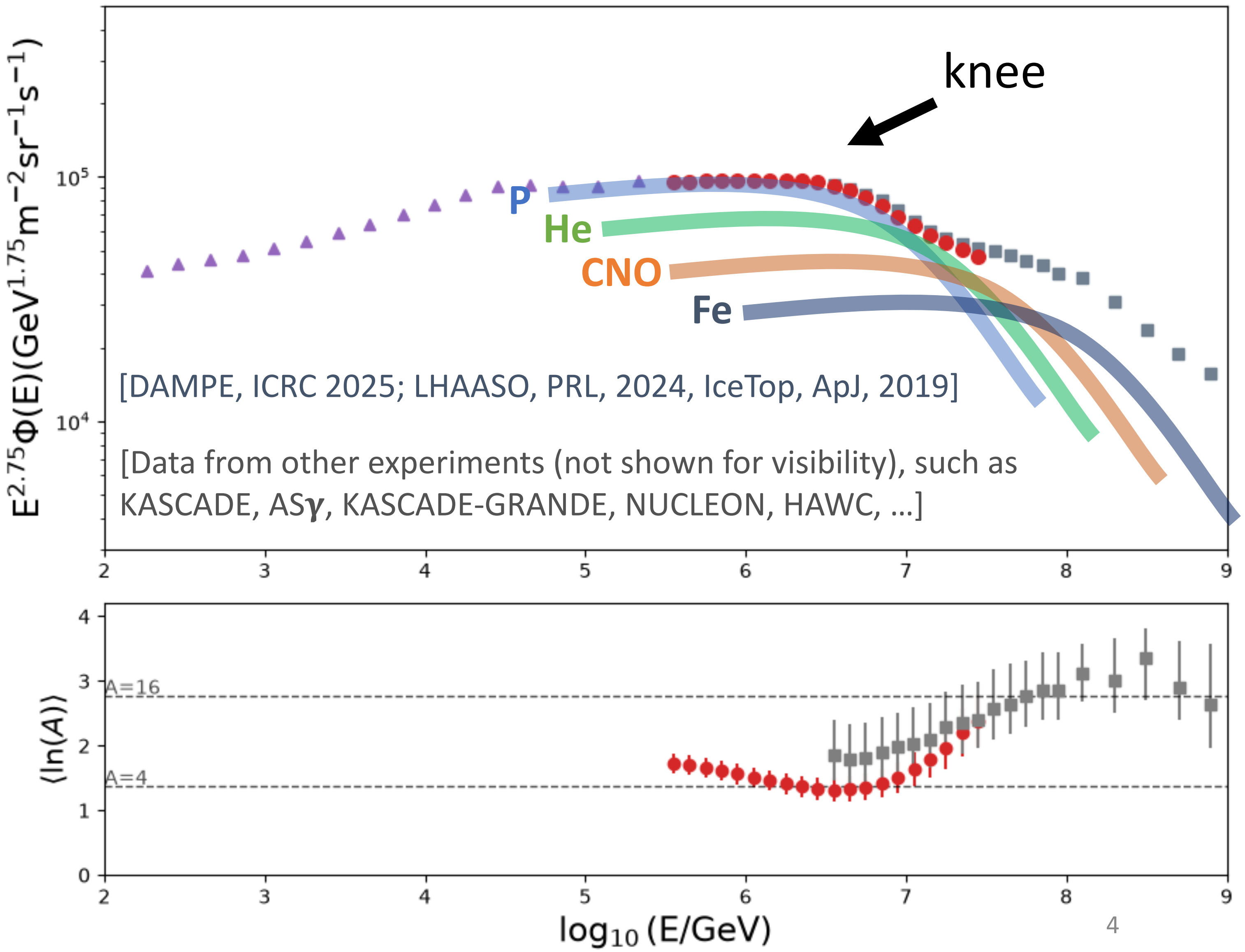

Origin of CR knee

Insights from cosmic ray proton and helium observation

Origin of CR knee: proton and helium spectrum

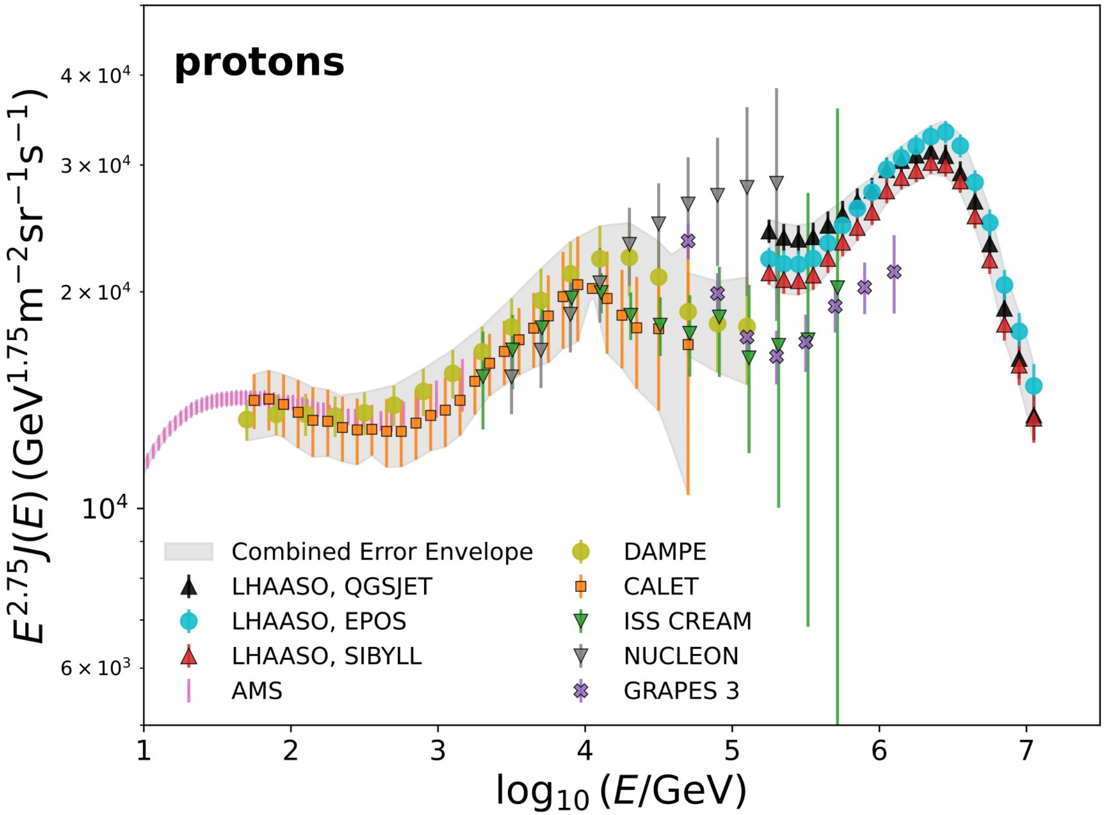

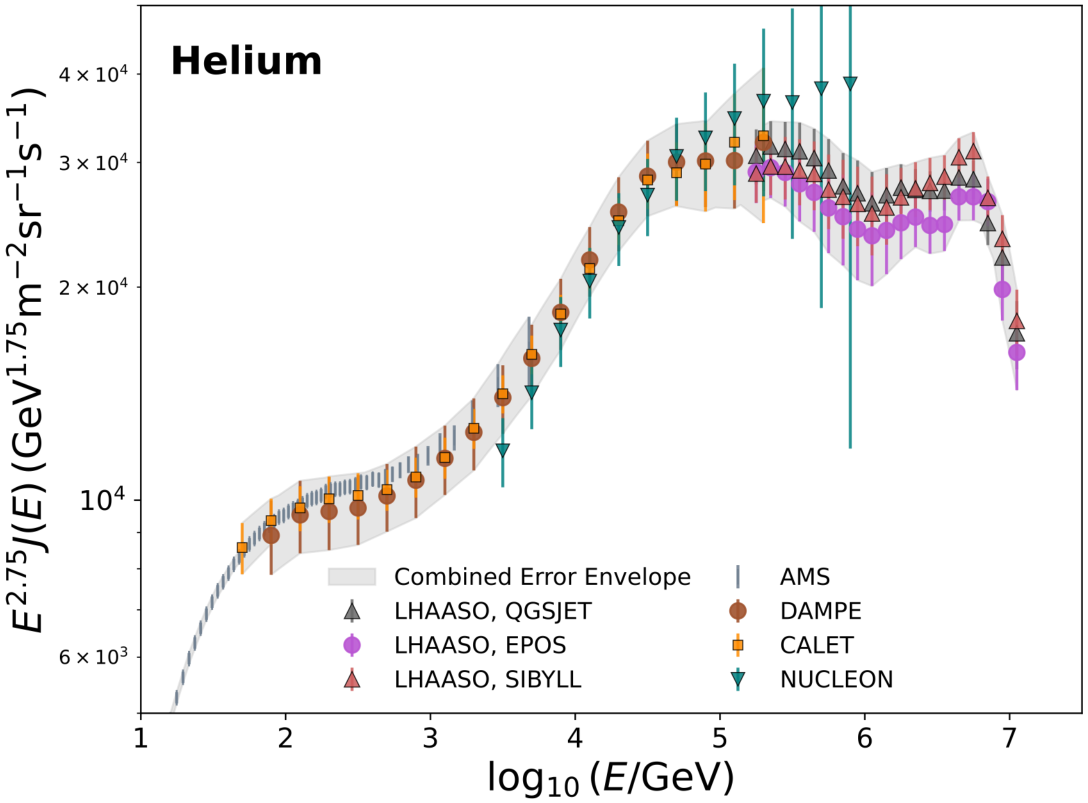

- The wealth of high-precision measurements accumulated over the past decade has established a complex structure in the CR proton and helium spectra

- Around 100 TeV, the uncertainty bands broaden significantly, reflecting the effects of limited statistics in direct measurements, focuses on a representative subset of proton and helium measurements reported by the AMS-02, DAMPE, LHAASO

Origin of CR knee: proton spectrum

Galactic CR proton spectrum is not single powerlaw, but show complex harderning and steeping features

- The all-particle ``knee'' is related to the steeping of the proton spectrum
- The proton spectral index above ``knee'' is ~3.5, steeper than the all-particle spectral index ~ 3.1
- The steeping in the proton spectrum may reflects the maximum acceleration energy of Galactic PeVatrons

[Proton data from CALET, GRAPES-3 not shown for visibility]

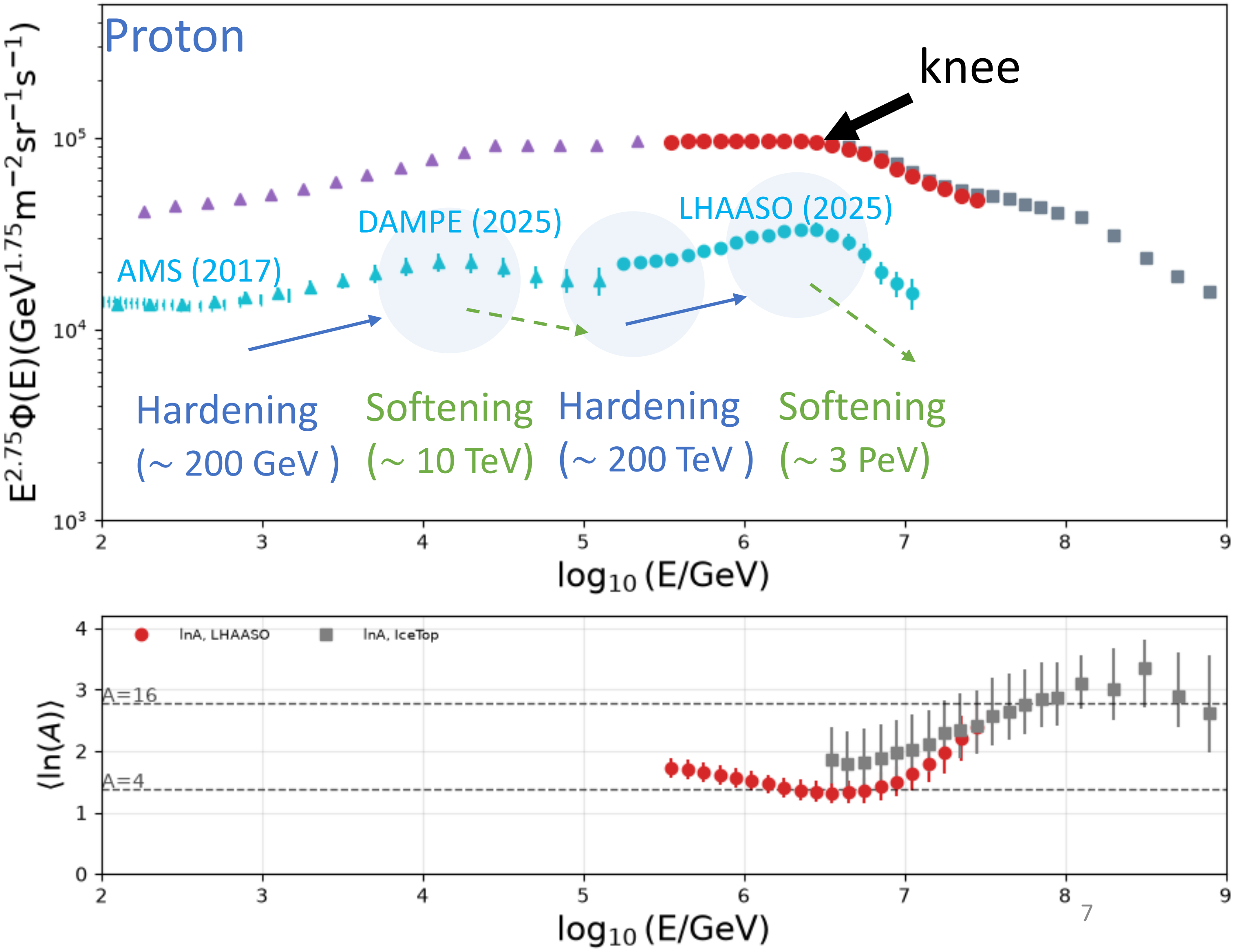

Origin of CR knee: helium spectrum

Galactic CR proton spectrum is not single powerlaw, but show complex harderning and steeping features

- The helium spectral index above ``knee'' steeper than the all-particle spectral index
- The flatter all-particle index is maintained by the contributions of heavier nuclei (like CNO, Fe) whose knees occur at even higher energies
- Consistent with the standard picture where the all-particle spectrum is a superposition of different Species

[Proton data from CALET, IceTop not shown for visibility]

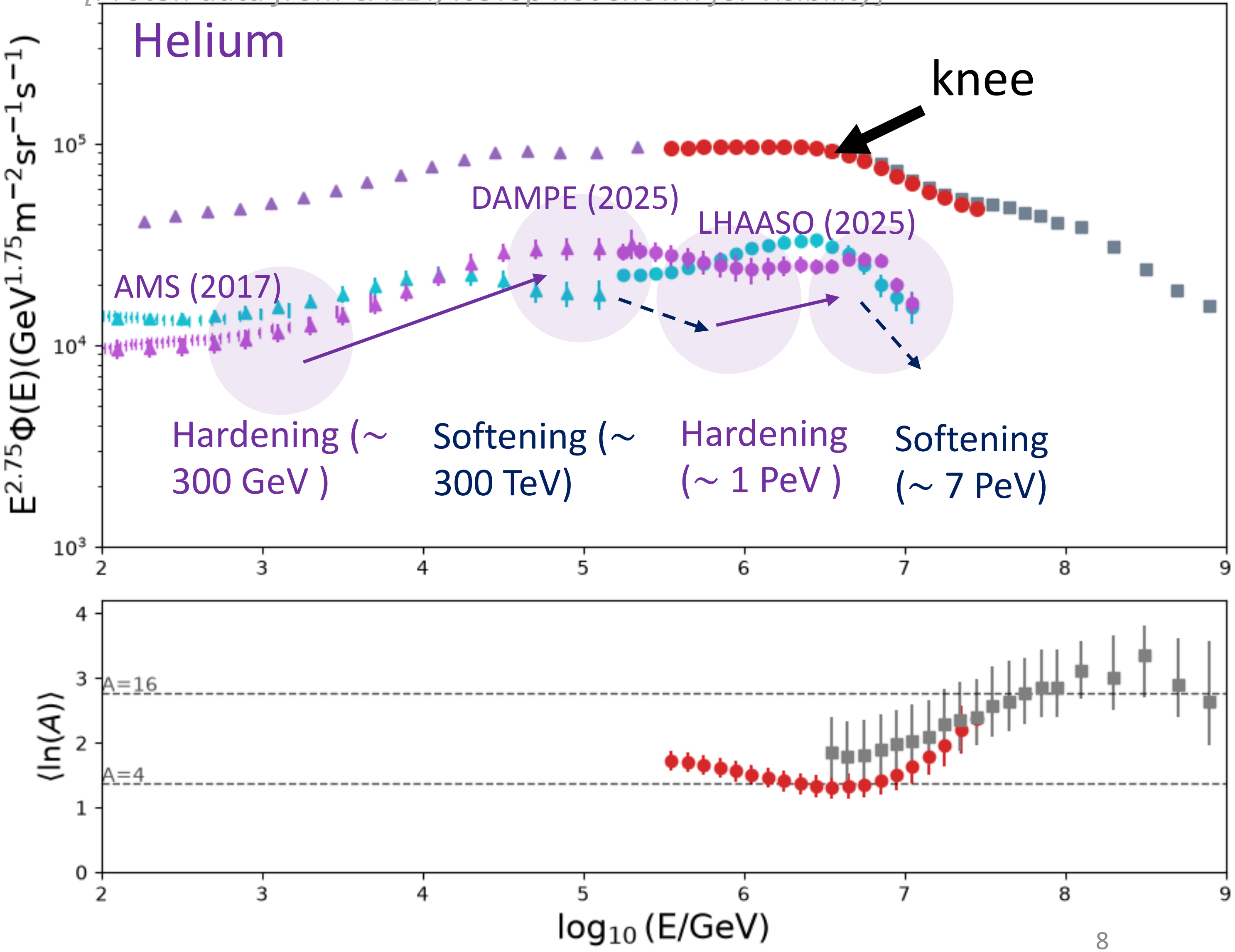

The sources of Galactic cosmic ray

Components inferred from observed proton and helium spectrum

A Minimal Interpretation of the Galactic Cosmic Ray

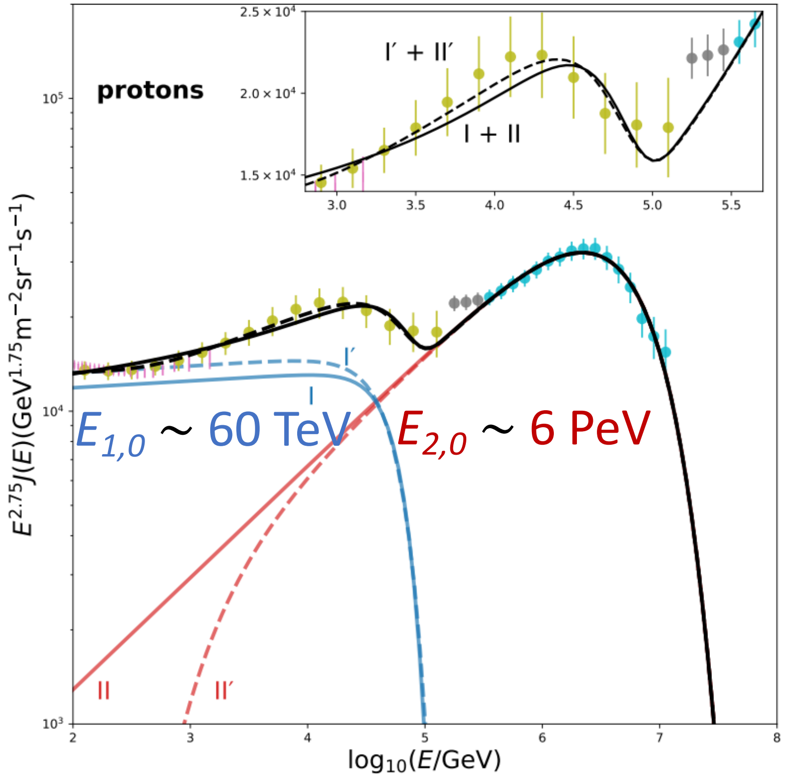

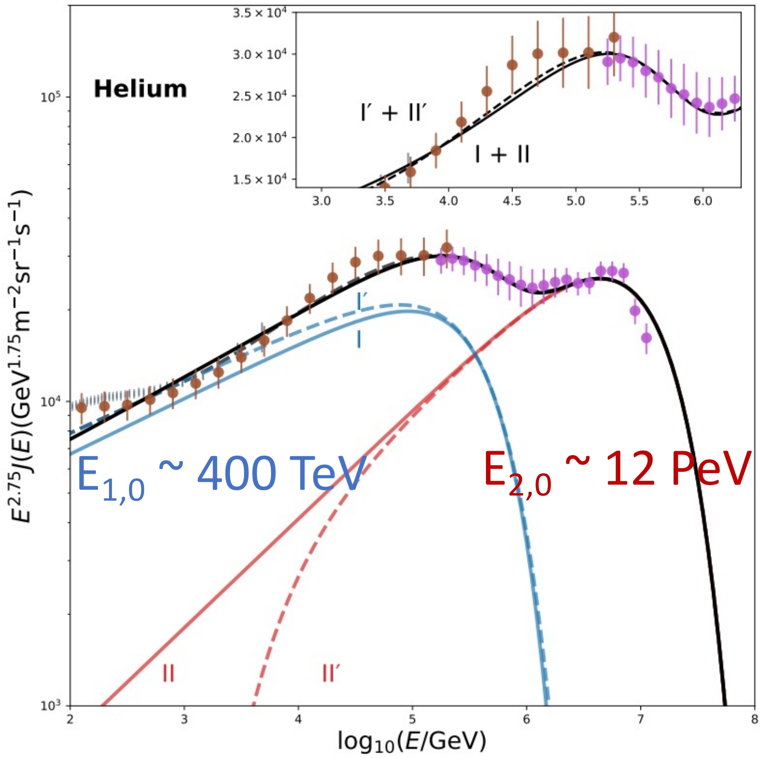

$$J_{\mathrm{tot}}(E) = J_1(E) + J_2(E)$$

$$J_i(E) = A_i\, E^{-\Gamma_i} \exp\left[-\left(\frac{E}{E_{i,0}}\right)^{\beta_i}\right]$$

A harder first helium component than that of the proton component, extending effectively to several hundred TeV

The second helium component scales with the proton spectrum as a function of rigidity

[Aharonian and BTZ, 2026, ApJ, arXiv: 2062.08223]

The “multi-TeV bump” arises from the transition between a low-energy component with a sharp cutoff at tens of TeV and a second, harder component naturally dominates above~100 TeV and extends to PeV energies

This approach requires neither nonstandard acceleration or propagation scenarios nor local effects such as the presence of a dominant nearby source

Proton to helium ratio

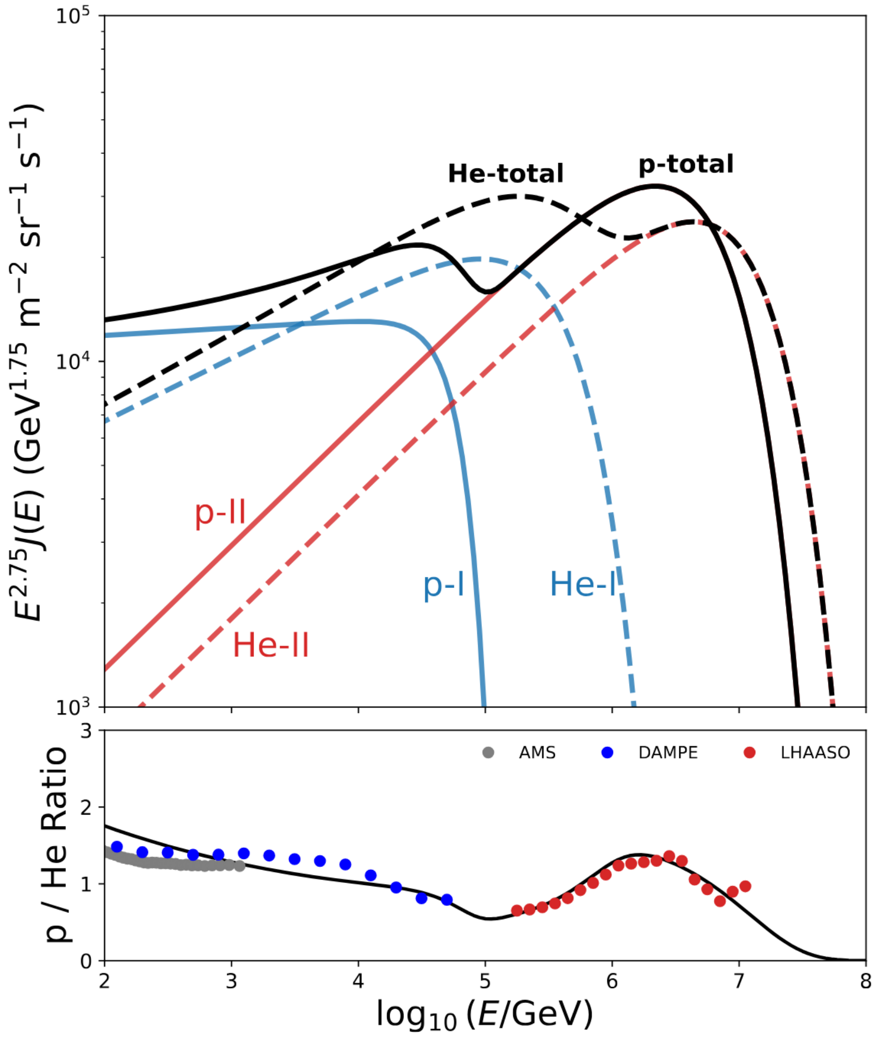

[Aharonian and BTZ, 2026, ApJ, arXiv: 2062.08223]

The differences between the proton and helium spectra provide a natural explanation for the behavior of the p/He ratio

Reproduces the main features : the decrease and subsequent recovery in the multi-TeV region arise from the transition between the two components

Astrophysical implications

The nature of the source populations that may contribute to the two distinct components identified in the spectral analysis

SNRs origin of the first component

SNRs as the dominant source population responsible for Galactic CRs

- Observations of SNRs oftentimes show power law spectra non-thermal emission of X-rays [*Reynolds, 2008*]
- Diffusive shock acceleration work in SNR's blastwave
  [*Krymsky12; Bell13; Axford, Lear and Skadron14; Blandford and Ostriker; 1977-78*]
- The locally observed energy density of cosmic rays can be explained if on average ~ 10% of the shock kinetic energy is converted to GCRs
  [*Strong ApJL, 2010*]

SNRs origin of the first component

- Relatively low cutoff energy (< 100 TeV) and super-exponential cutoff (beta > 2) for the first CR proton component

- Higher cutoff energy (< 100 TeV) and exponential cutoff (beta ~ 1) for the first CR helium component

SNR properties inferred from latest observations

W 51 C

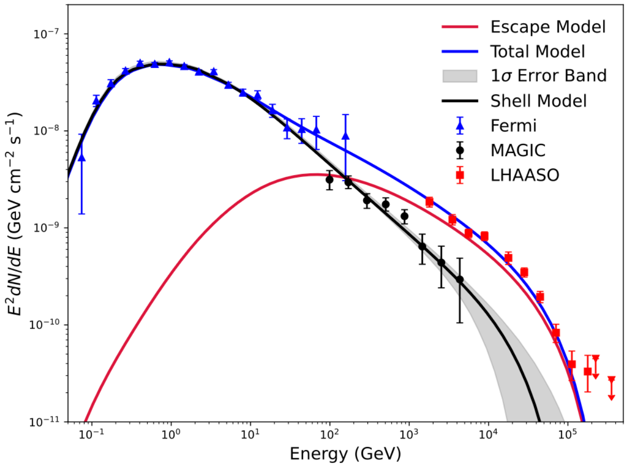

W44

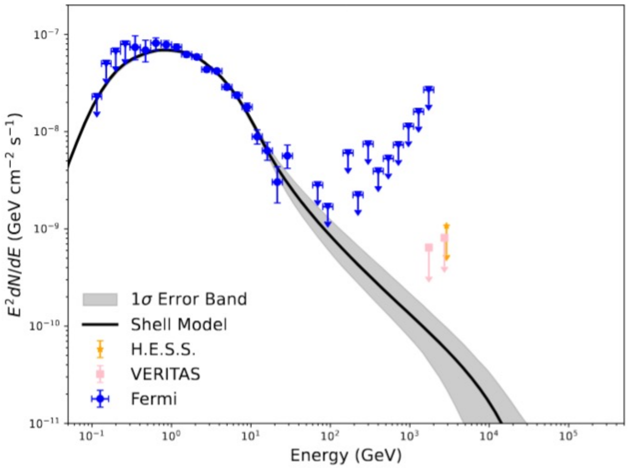

IC 443

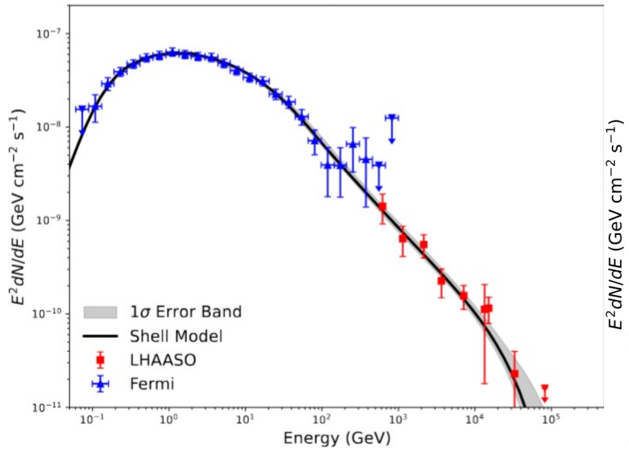

W28

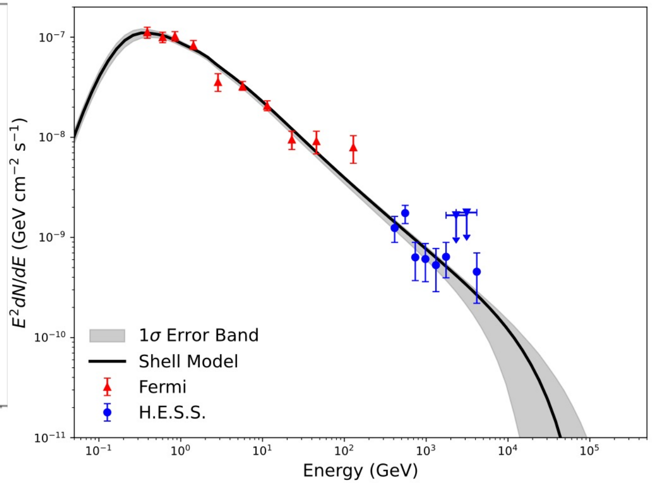

[Chen, BTZ, Xing & Liu, 2026, arXiv: 2608.18954] A time-dependent modeling of the gamma-ray emission from four SNRs

$E_{\rm max} = 164^{+345}_{-110}$ TeV, $s_{\rm cr} = 2.26^{+0.09}_{-0.08}$ $E_{\rm max} = 105^{+385}_{-83}$ TeV, $s_{\rm cr} = 2.25^{+0.06}_{-0.08}$ $E_{\rm max} = 375^{+327}_{-183}$ TeV, $s_{\rm cr} = 2.34^{+0.03}_{-0.04}$ $E_{\rm max} = 172^{+393}_{-128}$ TeV, $s_{\rm cr} = 2.21^{+0.05}_{-0.05}$

- Accelerated CRs are confined to a narrow range of α∼2.2−2.3
- The maximum proton energies are constrained to *E*p,max ∼ 100−300 TeV, although the constrains subject to large uncertainties, allowing values from∼50 TeV up to∼500 TeV

Galactic PeVatrons

Galactic PeVtron candidates:

Supernova remant (Some special or energetic SNRs? e.g., higher shock velocity; magnetic field amplification; Absence of UHE γ-ray detections from Cen A; Escaped CRs interact with nearby giant molecular cloud could be smoking gun)

Pulsar wind neuble (Extreme accelerator, however, no evidence of proton/ion acceleration or hadronic origin of gamma-rays)

Young Massive stellar cluster (Detailed theoretical studies indicate that reaching the PeV domain through stellar-wind interactions alone is highly challenging)

Microquasar (Several sources detected in UHE gamma-ray band, Powerful PeV accelerators, evidence of hadronic interaction)

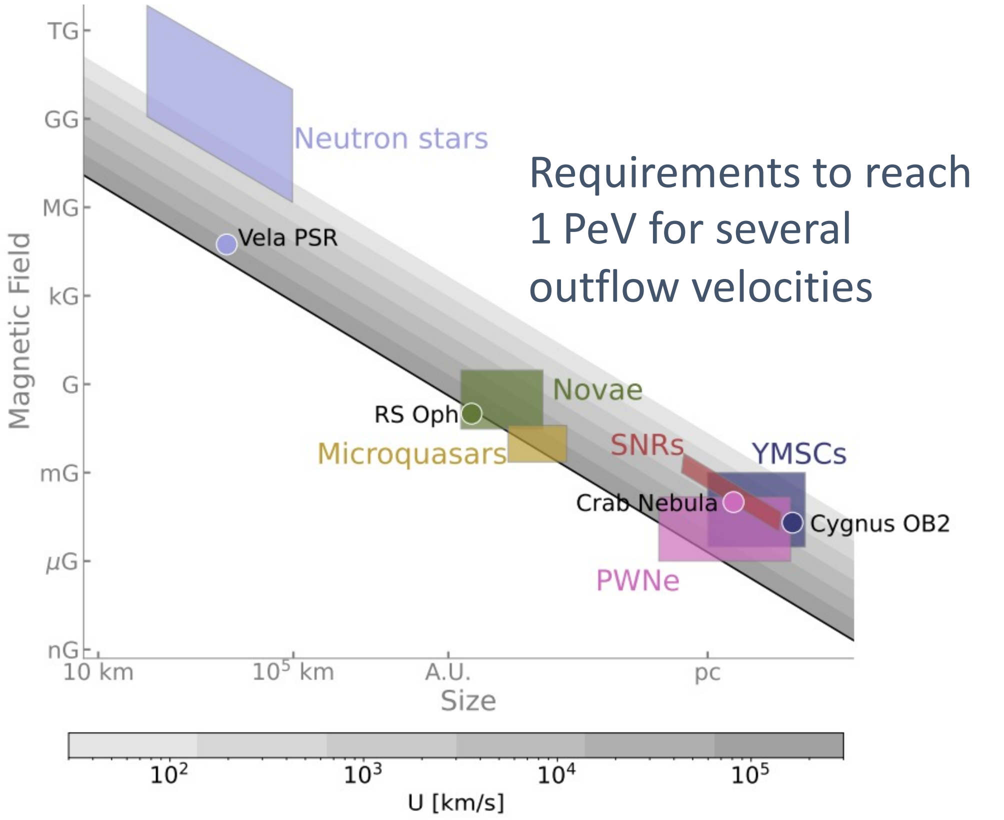

[de Ona Wilhelmi et. al., 2024]

$$E_{\rm max}^{\rm th} = Z \left(\frac{e}{c}\right) L\, U\, \mathcal{B} \approx 0.3\, Z \left(\frac{L}{\rm pc}\right) \left(\frac{U}{1,000\,{\rm km\,s^{-1}}}\right) \left(\frac{\mathcal{B}}{100\,\mu{\rm G}}\right) {\rm PeV}$$

Microquasars jets are efficient CR accelerators

Diffusive shock acceleration

Acceleration in jets or wind termination shock is possible, accelerated CRs typically show a power law spectrum with exponential cutoff

[E.g., Cooper et al, 2020; Perettil et. al., 2025; Wang et al. ApJL, 2025; Kaci et. al., 2025, arXiv:2510.01369]

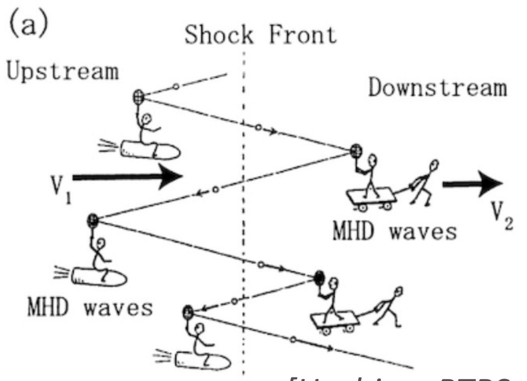

[Hoshino, PTPS, 2001]

Shear acceleration

- A class of the Fermi acceleration, has been suggested to be an efficient mechanisn to accelerate CRs
- Charged particles gain energy inside an ordered shear velocity field

[E.g., Berezhko and G. F. Krymskii, 1981; Earl, J. R. Jokipii, ApJL, 1988; Ostrowski A&A, 1990; Webb ApJ, 1989; Rieger, Universe, 2019, Seo et. al., ApJ, 2023; BTZ, Kimura & Murase, 2025, PRD; Wan et al, 2025]

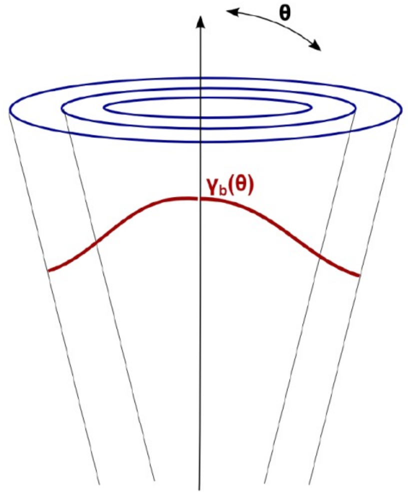

Rieger, Universe, 2019

Example: Physical properties of GRS 1915+105

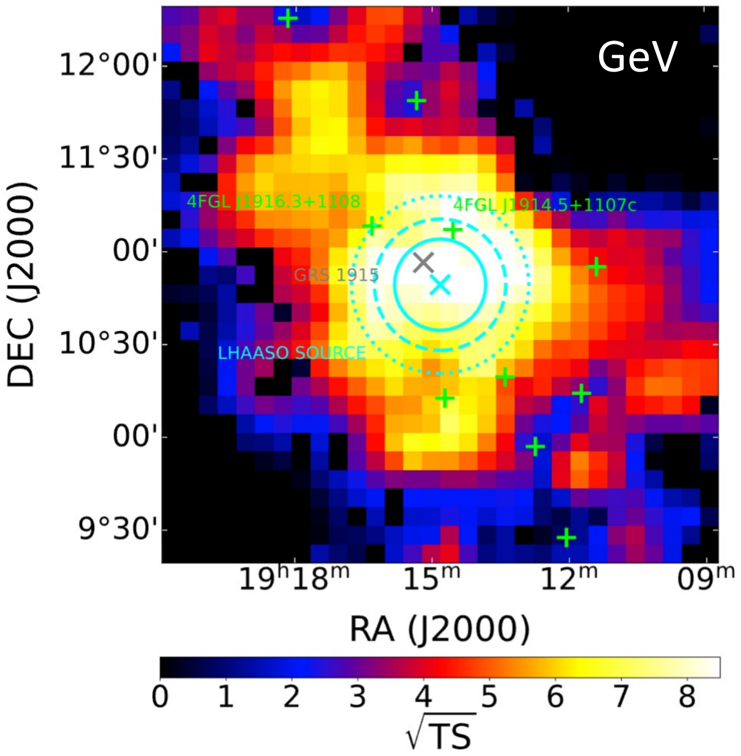

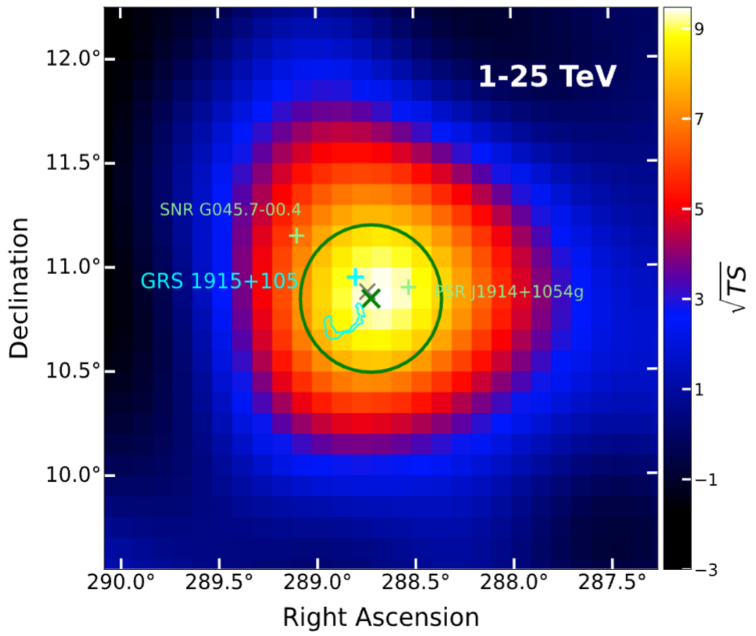

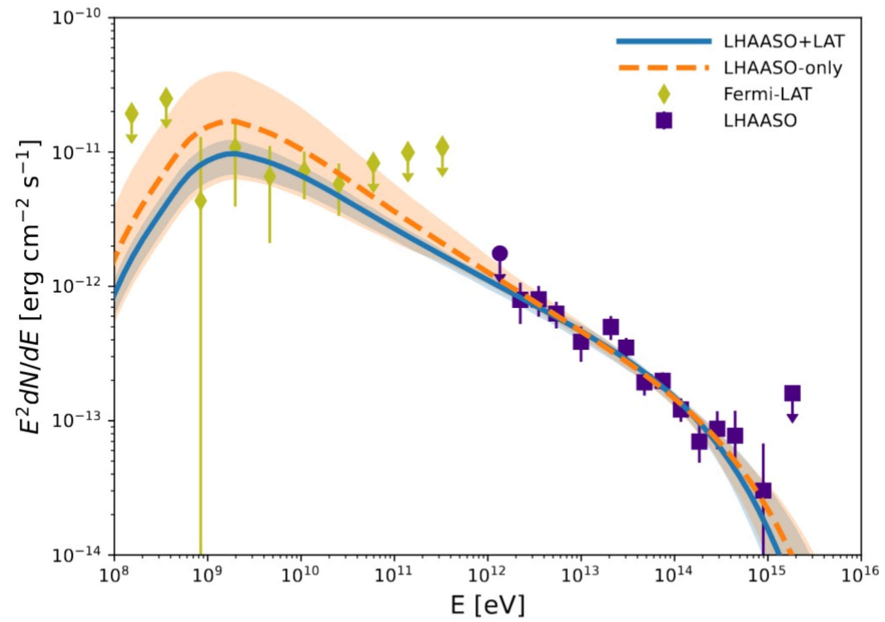

[LHAASO Collab., 2026, arXiv:2606.25054]

The broadband spectrum and dense local environment favor a hadronic origin through neutral pion decay

The inferred CR spectrum α~2.4 (pp) and maximum acceleration energy ~ 5 PeV (Harder acceleration spectrum α~2)

History of Milky Way accelerators

Microquasars are characterized by lower spatial densities, the local CR flux is inherently subject to stochastic fluctuations …

Co-author Shiqi Yu (University of Utah)

Cosmic ray clouds from microquasars in our galaxy

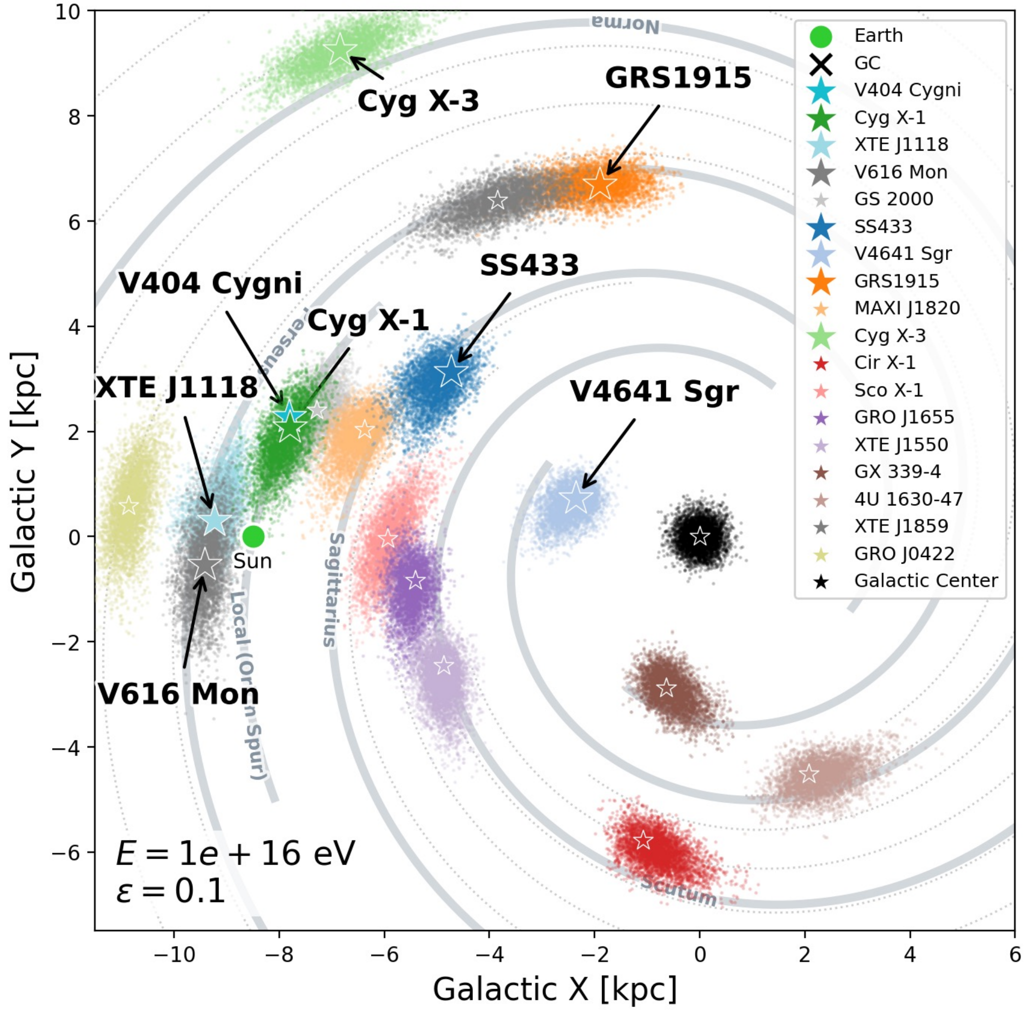

- llustration of the spatial distribution of 1 PeV cosmic rays (colored dots) from known Galactic microquasar locations (stars)

- The CR transport is influenced by the filamentary morphology of the Galactic magnetic field (gray spirals)

We employ constant diffusion with parallel coefficient to the regular magnetic-field direction as

$$D_{\parallel} = 6.1 \times 10^{28} (E/4\ \mathrm{GeV})^{1/3}\ \mathrm{cm}^2\ \mathrm{s}^{-1} \quad D_{\perp} = \varepsilon D_{\parallel}$$

In anisotropic diffusion scenario, the existence of regular GMF can results $D_{\parallel} > D_{\perp}$

Studies based on Galactic CR grammage constraints suggest an estimated range of ~0.01-0.1 from moderate to stronger cases

[e.g., Giacinti et. al., 2017, AL-Zetoun et. al., 2020]

[Zhang & Yu, 2026, arXiv: 2602.08940]

Anisotropic diffusion under Galactic magnetic field

Individual active sources exhibit significantly harder spectral features and higher flux levels

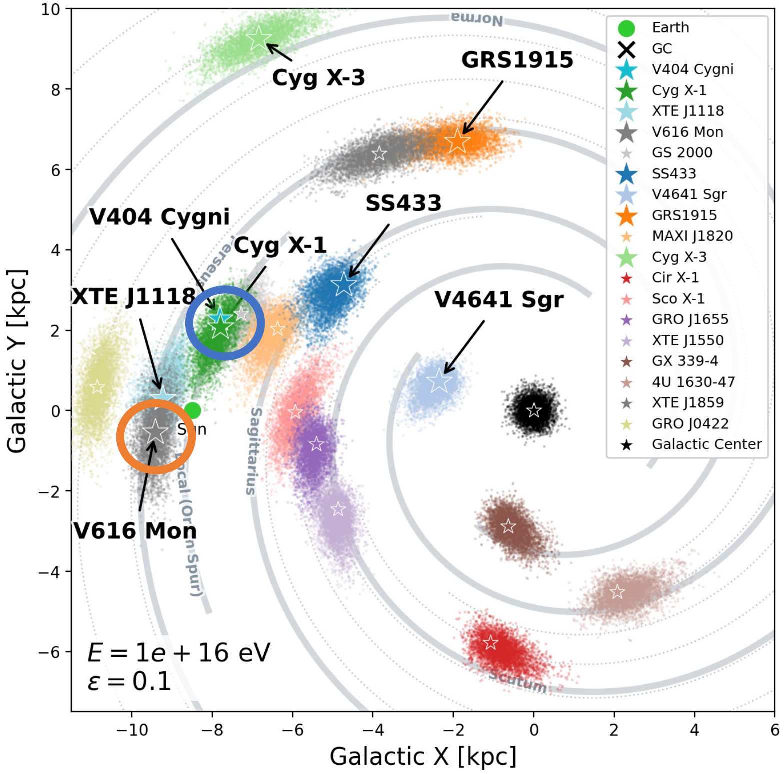

[Zhang & Yu, 2026, arXiv: 2602.08940]

Magnetic connection (epsilon = 0.01) has a stronger impact than physicaldistance to Earth

Injection with CR acceleration efficiency $\eta_{\rm cr} \sim 0.5\%$

$$Q = \eta_{\rm cr} L_{\rm Edd}$$

$$L_{\rm Edd} \simeq 1.26 \times 10^{39} (M_{\rm BH}/10\ M_\odot)\ {\rm erg\ s^{-1}}$$

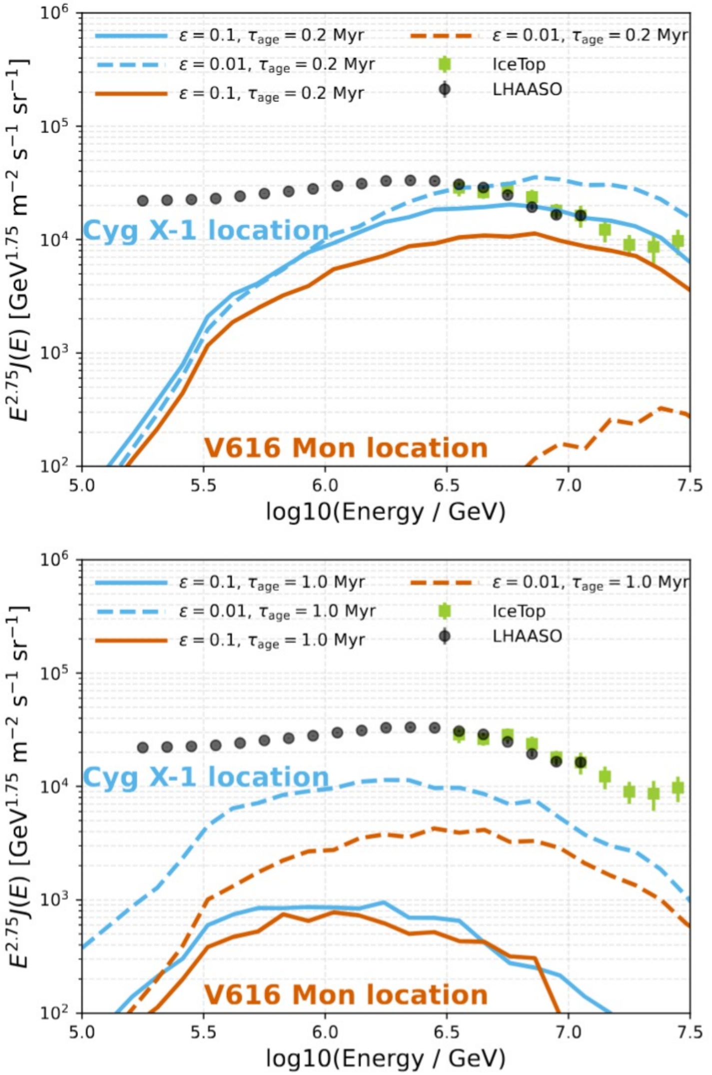

FIG. 2. Predicted CR spectra from Cyg X-1 and V616 Mon locations against data, comparing $\varepsilon = 0.1$ (solid), 0.01 (dashed), $\tau_{\rm age} = 0.2$ Myr (top), and 1 Myr (bottom), assuming Model A with $M_{\rm BH} = 10\,M_\odot$, $\tau_{\rm dur} = 0.2$ Myr, and $\eta_{\rm cr} = 0.005$.

The escaping CR proton spectrum taken from Model A of *[BTZ, Kimura & Murase, 2025, PRD, arXiV: 2506.20193]*

Random sampled Microquasar population

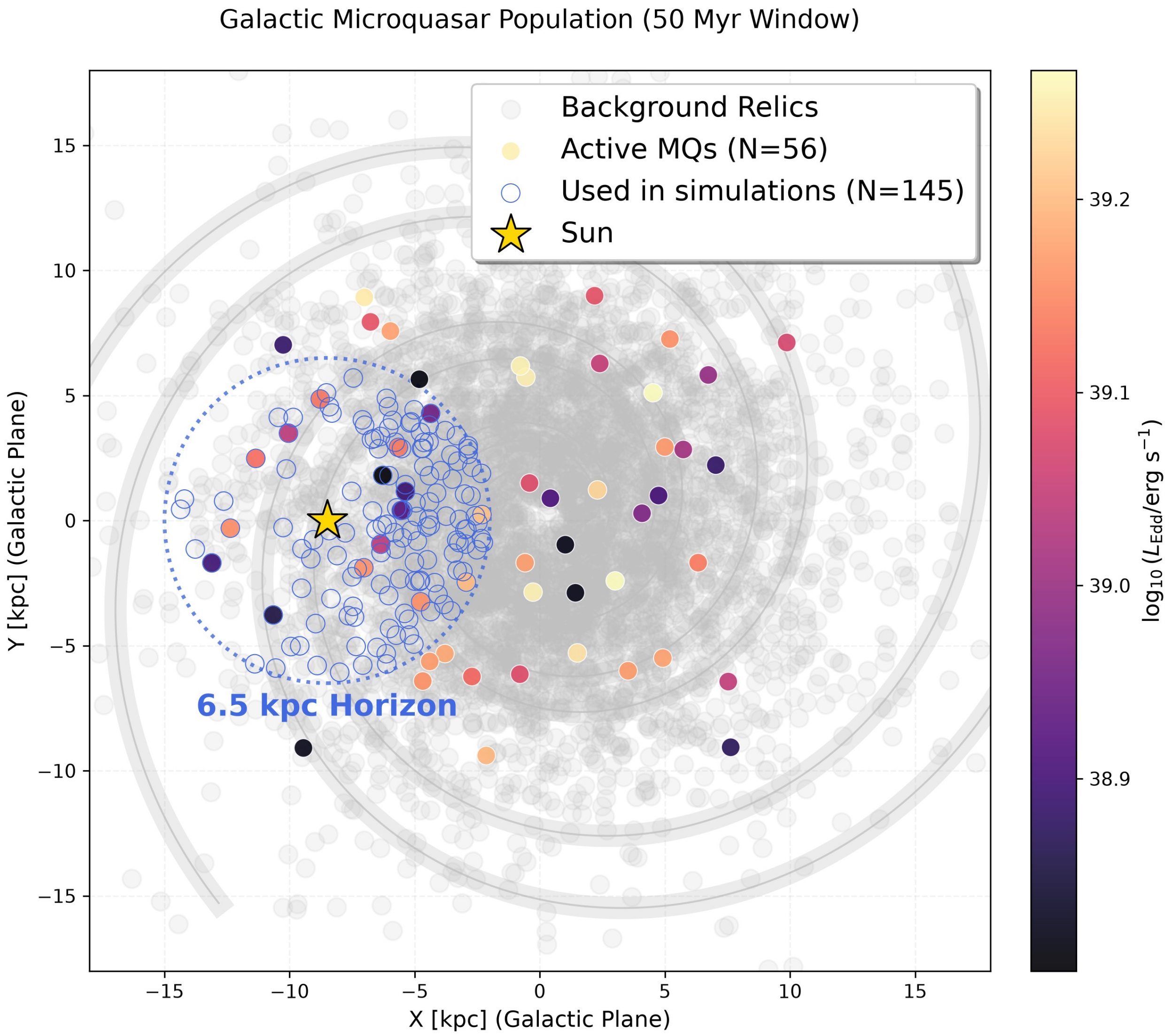

To account for spatial and temporal variance in the local microquasar population, we simulate an ensemble of 200 MC realizations using independent random seeds.

TABLE S2. Parameters used in the microquasar catalog generation and CRPropa simulation setup.

Parameter (Symbol)	Value / Distribution
Constants	
Birth Rate	1×10^{-4} yr^{-1}
CR Loading Efficiency (η_{cr})	0.1
Simulation Cutoff	6 Myr & non-active
Sample Ensembles	
Lookback Time ($t_{lookback}$)	$\mathcal{U}(0, 50)$ Myr
Jet Duration ($t_{duration}$)	$\mathcal{U}(0.1, 1.0)$ Myr
Black Hole Mass (M_{BH})	$\mathcal{U}(5, 15)$ $M_\odot$
Galactocentric Radius (r_{gc})	Green15
Vertical Height (z_{gc})	$\pm$Exp($h_z = 0.15$ kpc)
CRPropa Simulation	
Injected Primary	protons
Energy Range	[100 TeV, 100 PeV]
Energy Bins	21 (log-spaced)
Particles per Bin	25,000

[Zhang & Yu, 2026, arXiv: 2602.08940]

Fit proton bump data

- Both can reproduce the bump while PL has nicer low-energy extension

- The PeV bump in the CR proton spectrum is robust rather than being an occasional outlier

Model A (hard): $\eta_{\rm cr} \sim 0.3 - 1.5\%$

PL with index = 2: $\eta_{\rm cr} \sim 2 - 10\%$

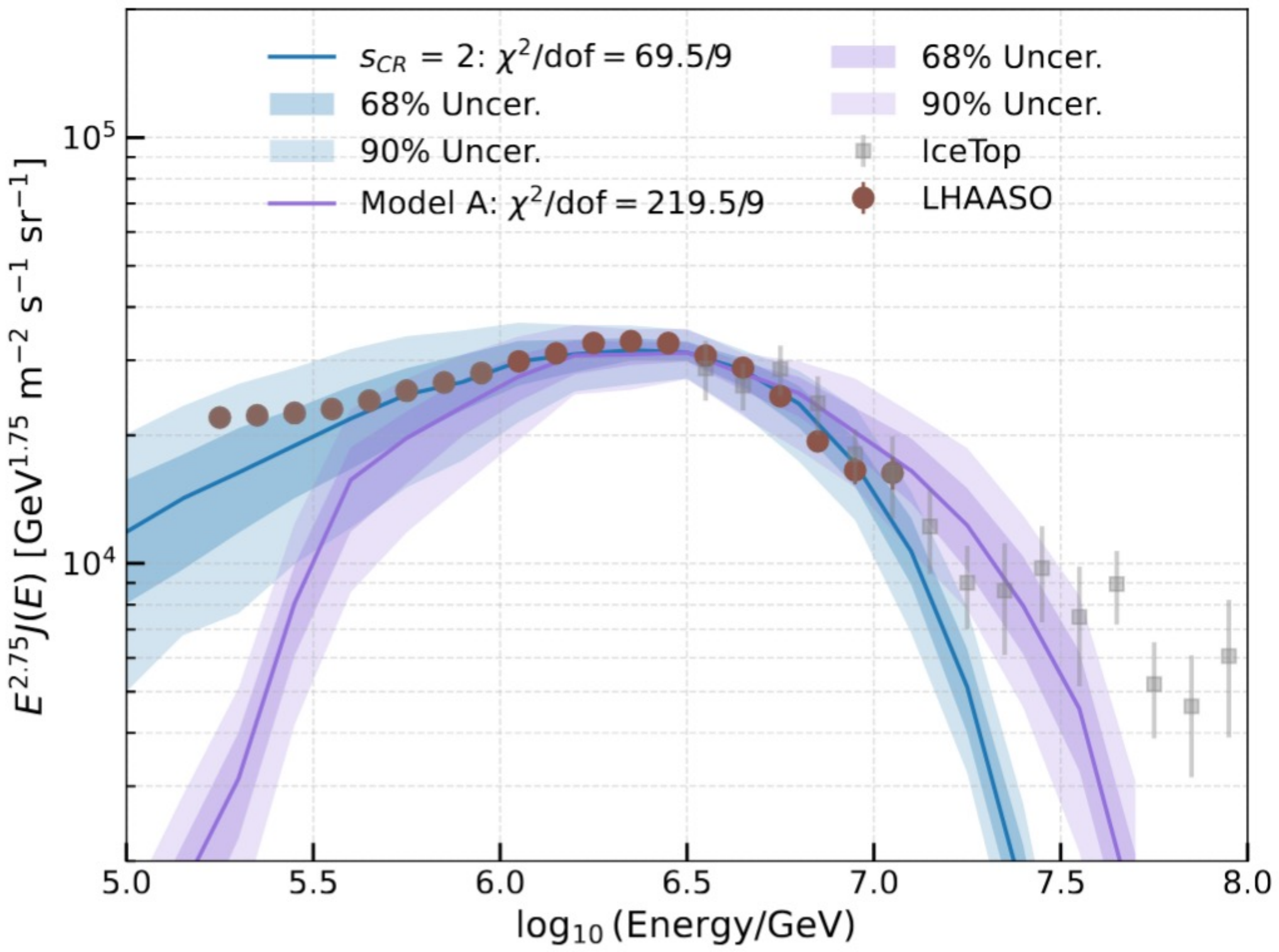

[Zhang & Yu, 2026, arXiv: 2602.08940]

Two realizations of source distributions

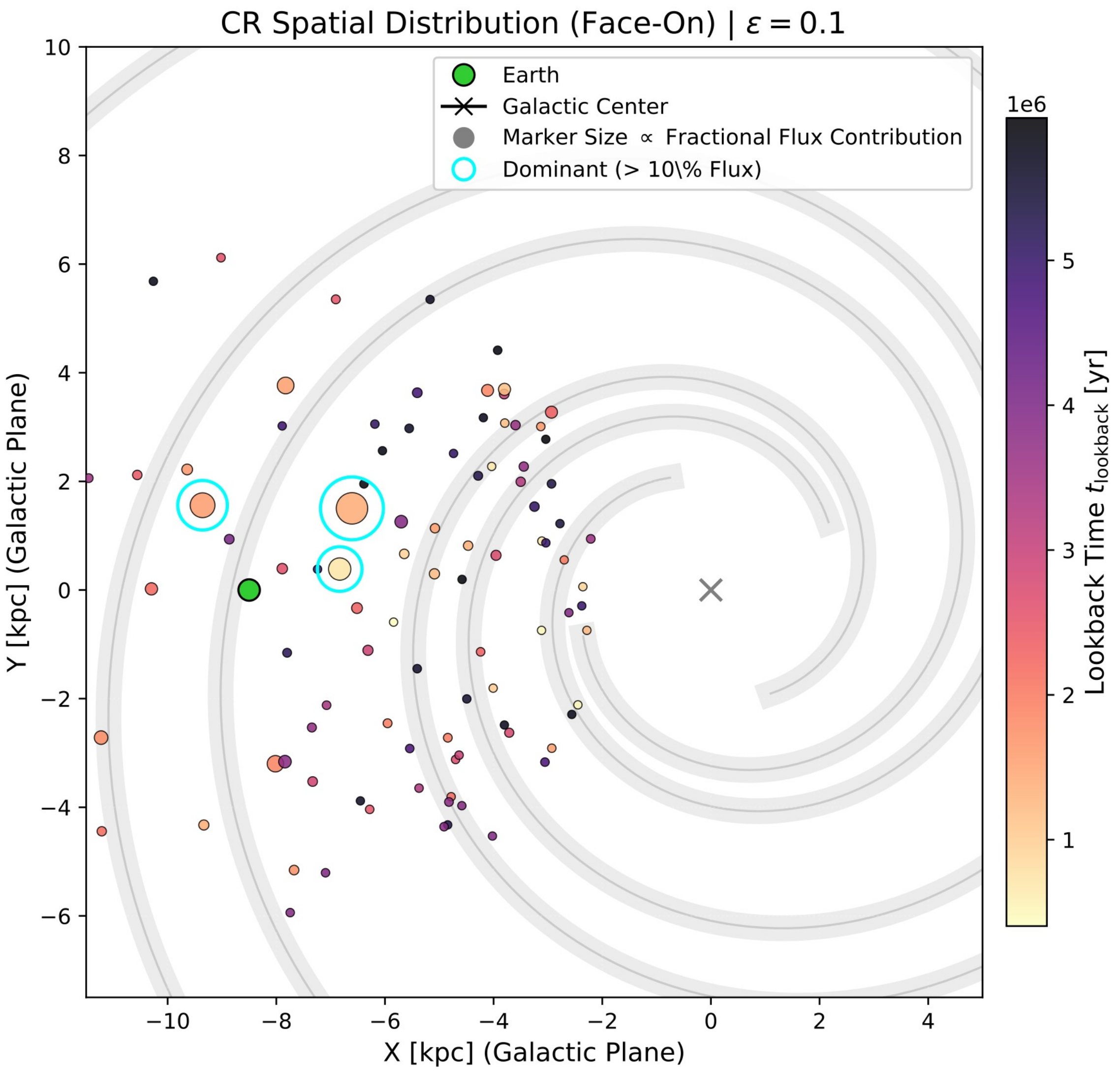

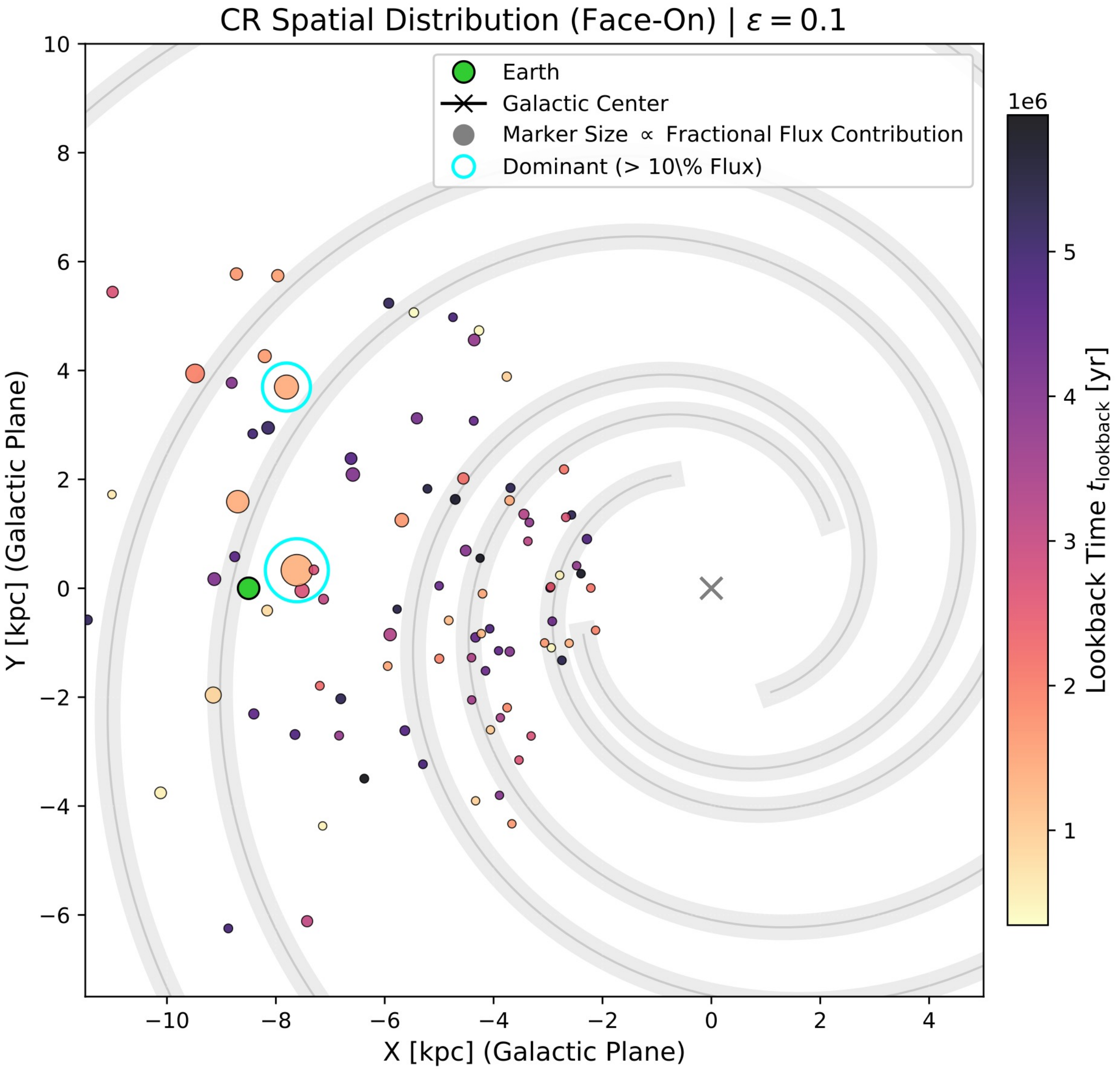

[Zhang & Yu, 2026, arXiv: 2602.08940]

Recent and nearby microquasar remnants

We calculate and rank the fraction of flux contributed from the individuals in each ensemble

- Usually no more than four sources are needed to explain 50% of the observed flux at 1 PeV

- The top ~10 sources contribute ~80%

The local PeV CR flux may not be a simple steady-state global average, but rather dominated by a few recent and nearby microquasar remnants

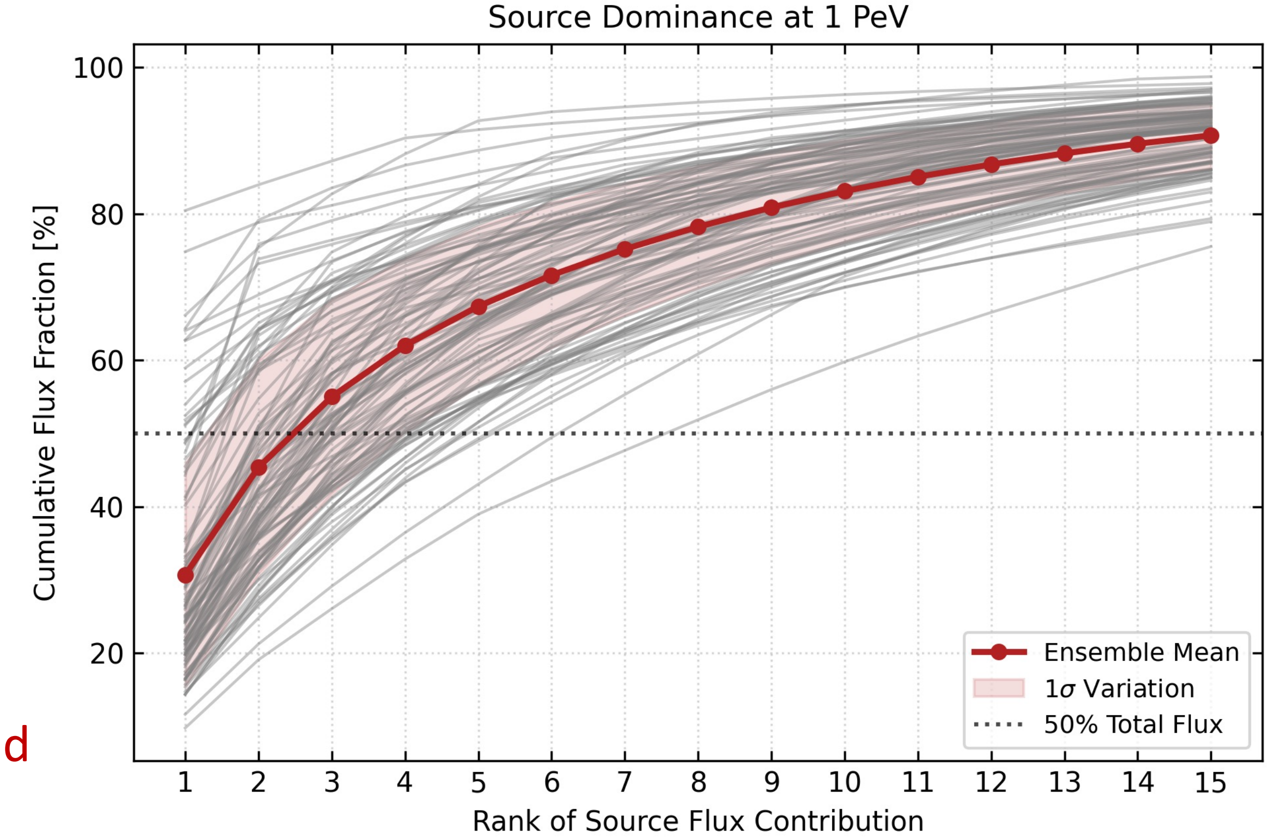

Cumulative fraction of the local CR flux at 1 PeV as a function of source rank, with sources ordered by their individual flux contributions

[Zhang & Yu, 2026, arXiv: 2602.08940]

Effects of source radial distribution

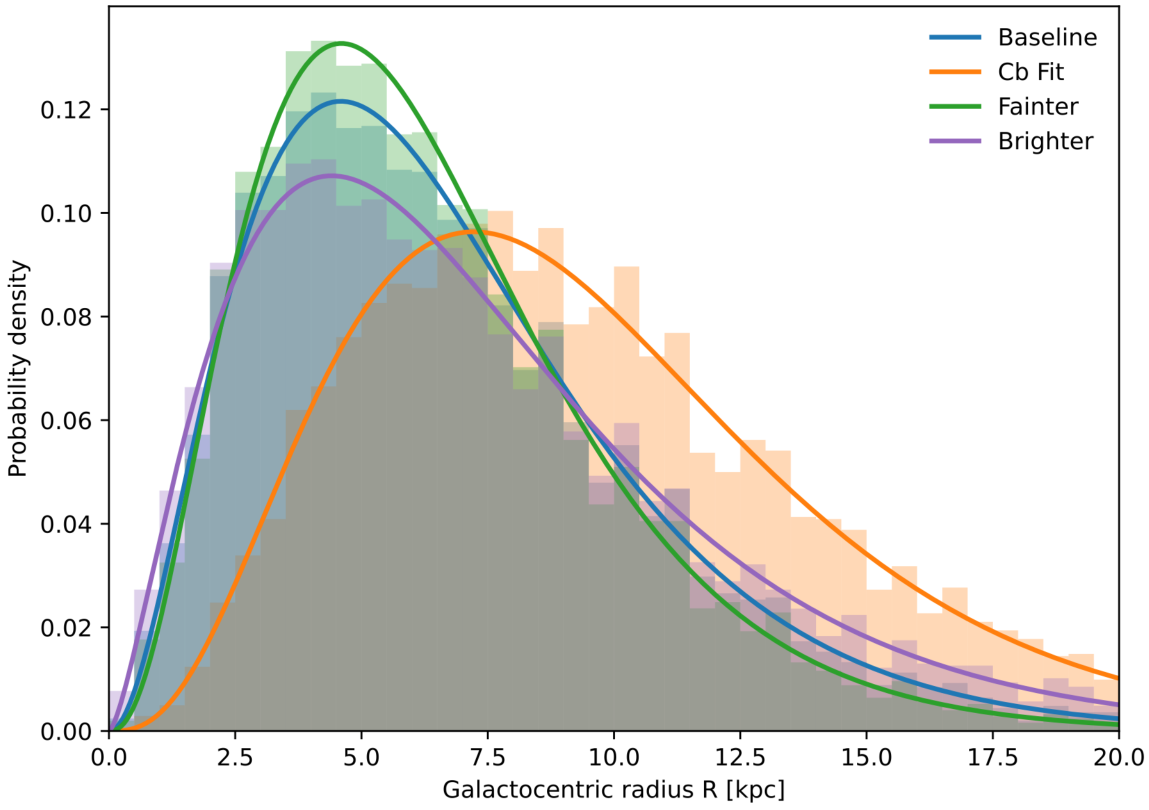

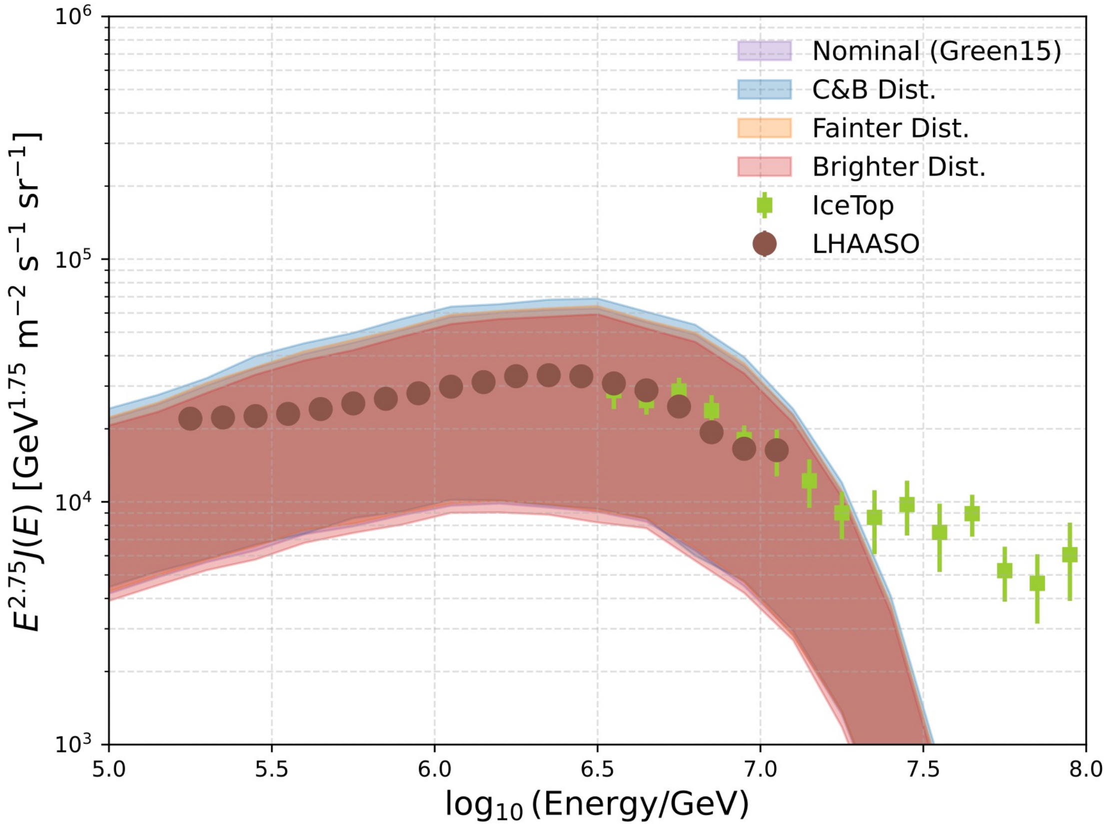

We test three more source distributions and show that their impacts on our predicted CR spectra is negligible

[Zhang & Yu, 2026, arXiv: 2602.08940]

Constraints from Galactic diffuse measurements

Secondary gamma-rays and neutrinos are produced from hadronic (*pp*) interactions between CRs with ambient gas

CR fit results yield a Solar neighborhood average, likely would miss the Galactic-level fluctuations can be traced by neutrinos and gamma rays → need multi-messenger constraints.

Galactic diffuse VHE gamma-ray and neutrino emission

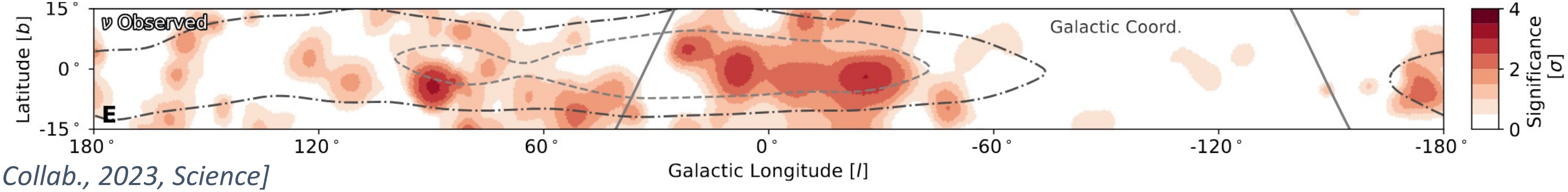

[IceCube Collab., 2023, Science]

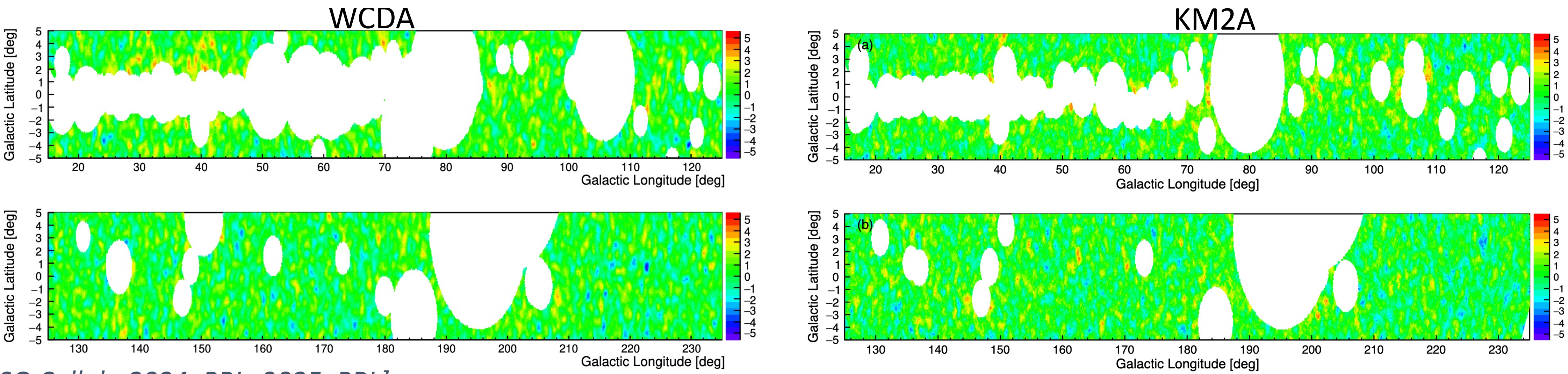

[LHAASO Collab, 2024, PRL; 2025, PRL]

- Gamma-rays (diffuse + unresolved src including leptonic process) v.s. neutrinos (diffuse + all src)
- CRs observed at Earth mainly from nearby sources, while diffuse gamma rays and neutrinos needs to account for sources across the whole galaxy

GCR source modeling

Injection spectral parameters for MQs and SNRs follow [Aharonian & Zhang, 2026 ApJ]

Protons and helium nuclei are injected and propagated independently

Heavier nuclei are scaled to helium following rigidity dependence

R-distributions from [Green 2015, MNRAS, 454, 1517]

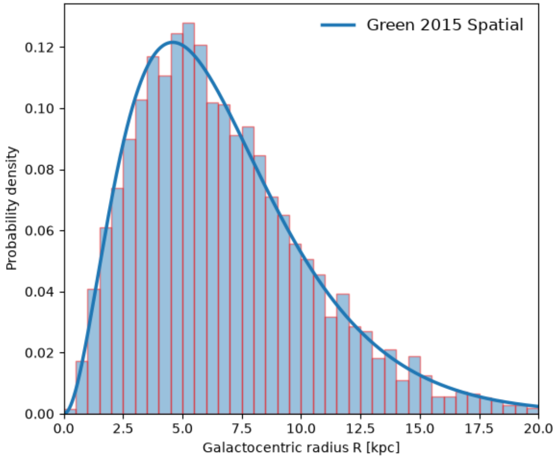

Table 2. Parameters for Population Distributions and CR Injection of MQs and SNRs.

Source	MQ	SNR
Shared Parameters		
Radial Distribution Parameters	$\alpha = 1.09, \quad \beta = 3.87$	
Time Window ($\Delta t_{\rm win}$)	50 Myr	
Pivot Height (h_z)	0.15 kpc	
Solar System Radius ($R_\odot$)	8.5 kpc	
Max. Lookback	20 Myr	
Distinct Parameters		
Birth Rate ($\mathcal{R}$)	1×10^{-4} yr^{-1}	$1/30$ yr^{-1} [a]
Jet Duration ($\tau_{\rm dur}$)	Uniform(0.1, 1.0 Myr)	–
CR Injection Index (s)	2.0	2.4 (2.24) for p (He)
CR Maximum Energy (s)	6 PeV	68(468) TeV for p (He)
Mass / Kinetic Energetics	$M_{\rm BH} \sim$ Uniform(5.0, 15.0) $M_\odot$	$\frac{E_{\rm SN}}{\rm erg} \sim$ Log-Norm(50.5, 0.53^2) [b]

CRs escape (τ_{esc}< 1 Myr at E > 1 TeV) prior to significant pp loss with τ_{loss}~ 50/(n_{gas}/1cm^{-3}) Myr and reach steady state << 20 Myr

[Yu & Zhang, 2026, arXiv: 2608.22374]

Population distribution

SNR

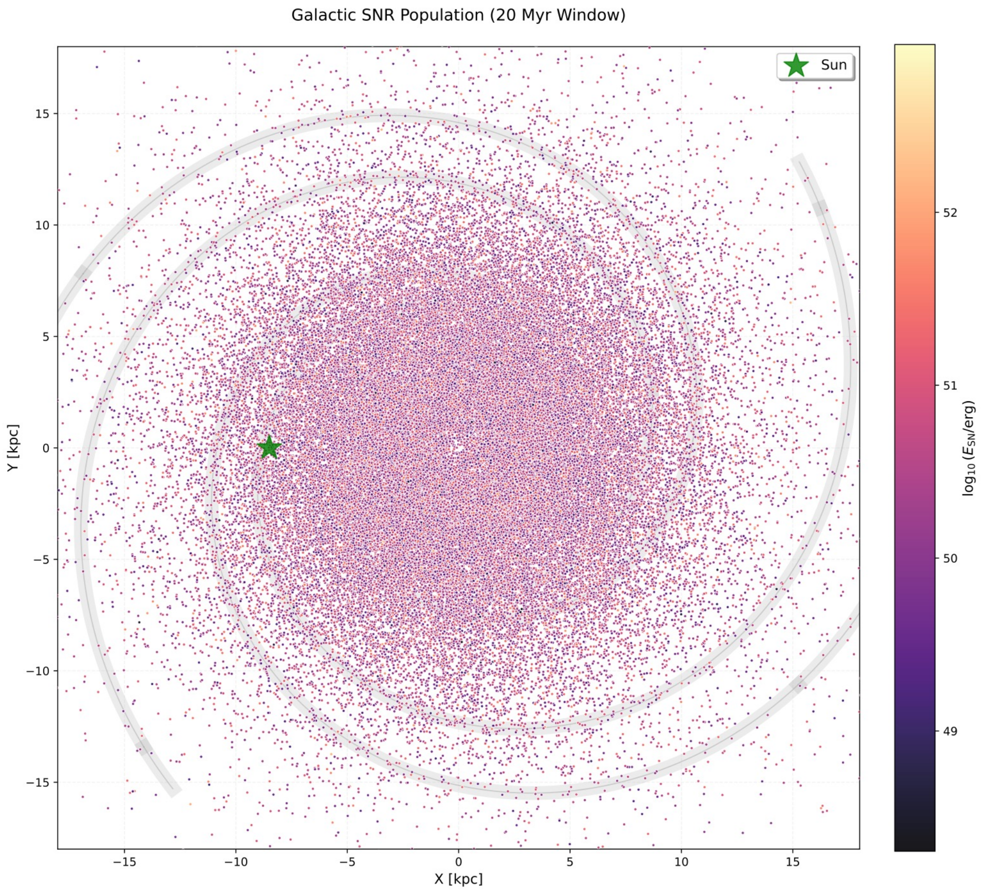

SNR spatial distribution shown with 10% sample [Green 2015]
Event rate: 1/30 yr

Microquasar

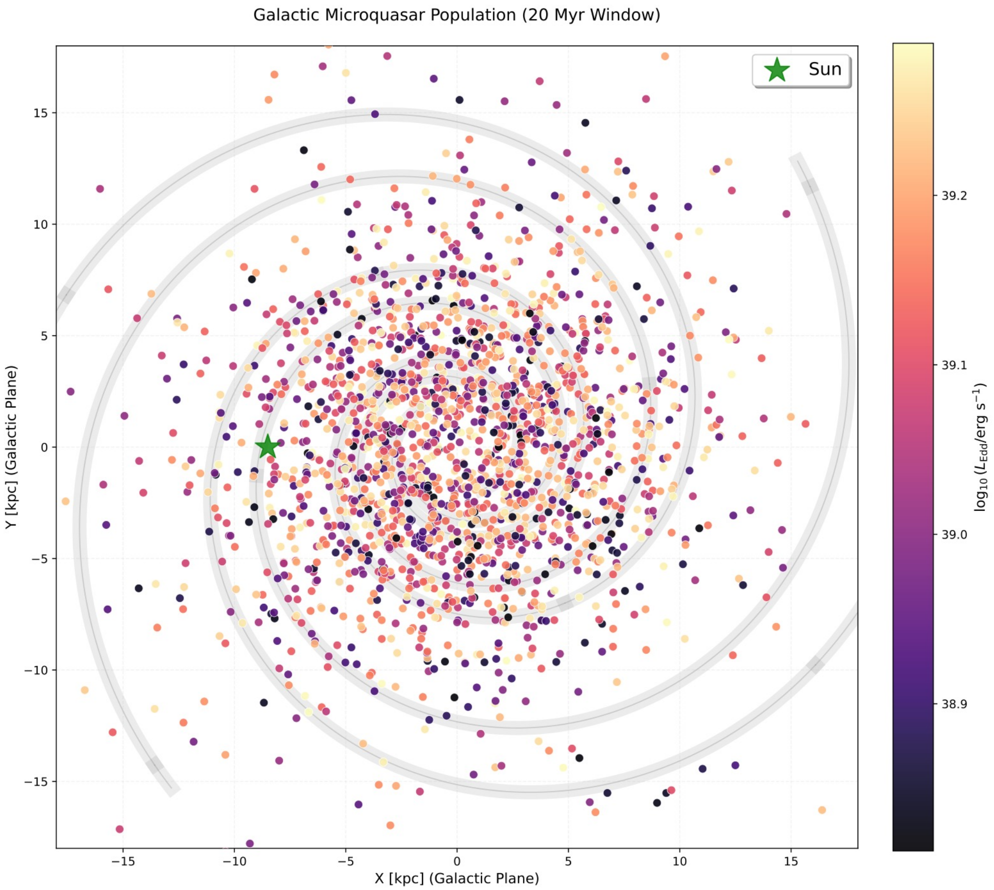

Microquasar spatial distribution [Green 2015]
Event rate: 1/10000 yr

[Yu & Zhang, 2026, arXiv: 2608.22374]

GCR diffusion

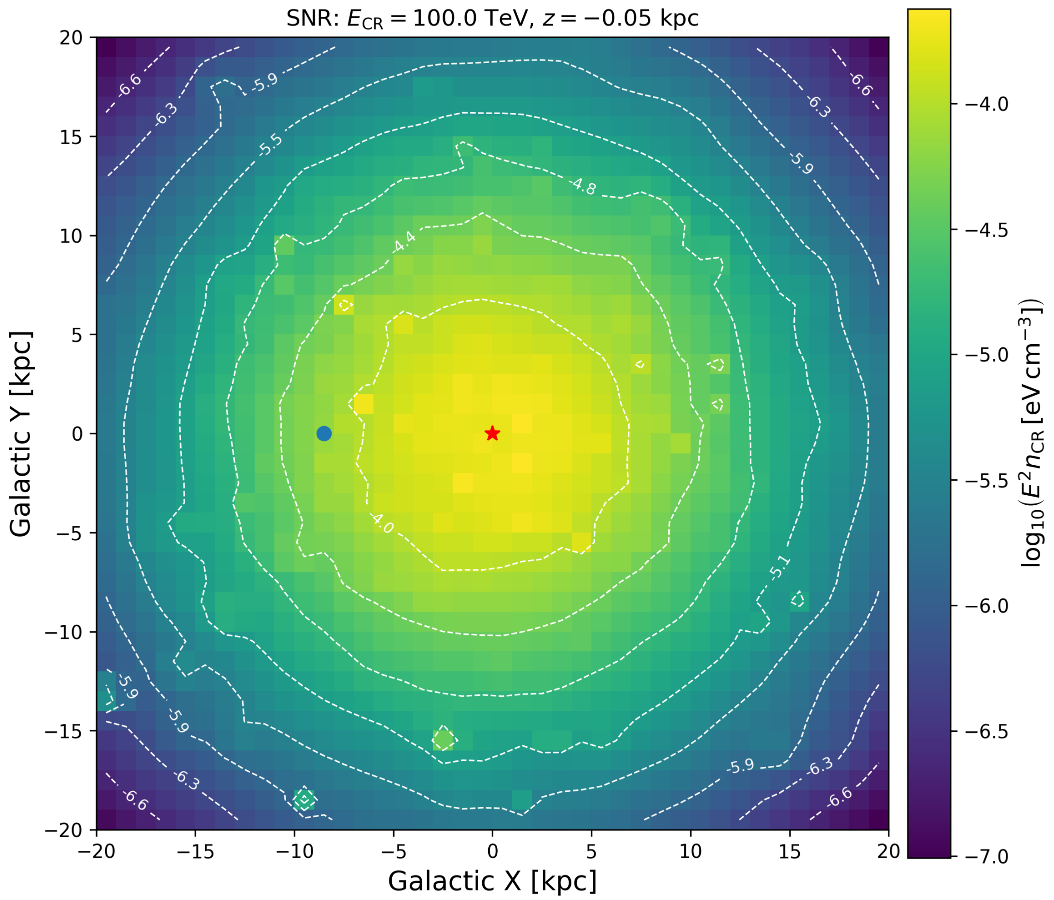

Illustration of steady-state CR density distribution of SNR at z=-0.05 kpc

Isotropic diffusion with constant diffusion coefficient, solving Green function:

$$n_{\rm cr}(E, \mathbf{r}, \tau_{\rm lookback}) = L_{\rm cr} \int_{\tau_{\rm min}}^{\tau_{\rm lookback}} \mathcal{P}(\mathbf{r}, E, \tau)\, d\tau$$

$$\mathcal{P}(\mathbf{r}, z, E, \tau) = \frac{1}{(4\pi\, D(E)\, \tau)^{3/2}} \exp\left(-\frac{r^2}{4D(E)\tau}\right) \mathcal{V}(z, \tau, E)$$

With free-escape boundary at +/- 4 kpc using Blasi & Amato 2011 methods

[Yu & Zhang, 2026, arXiv: 2608.22374]

3D Interstellar Radiation and Gas Distribution

Line-of-sight (LOS) integrations over gas and photon maps to estimate resulting **ν** and γ-ray emission

- **pp and He-p interaction** with gas nuclei via AAFRAG [Comput.Phys.Commun. 245 (2019) 106846], with heavier nucleus scaled by 1.42 [Castro et. al., 2025]
- ***γγ* absorption** accounts for CMB, EBL, and ISRF photon fields [Vernetto & Lipari 2016, Robitaille 2012]

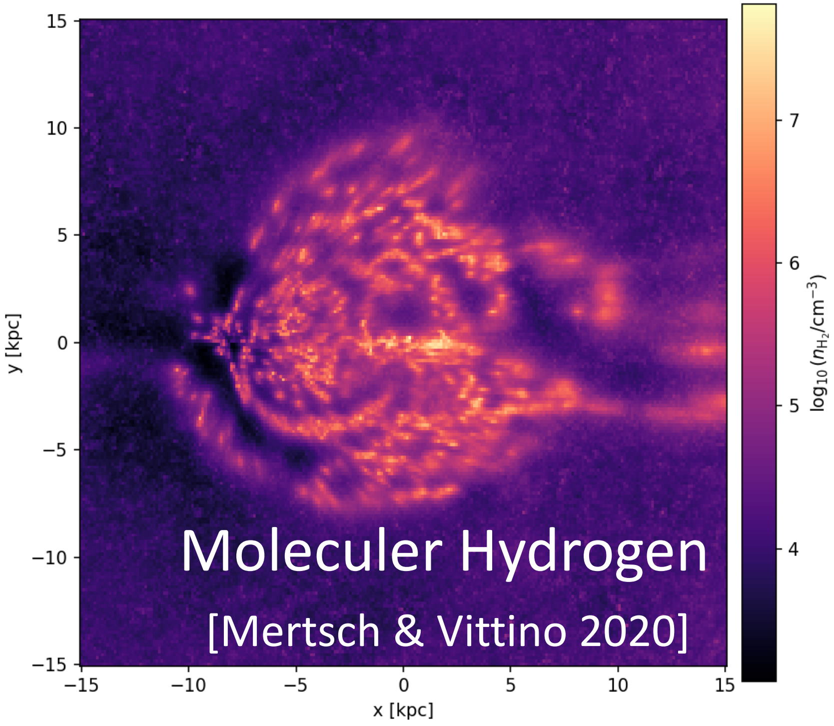

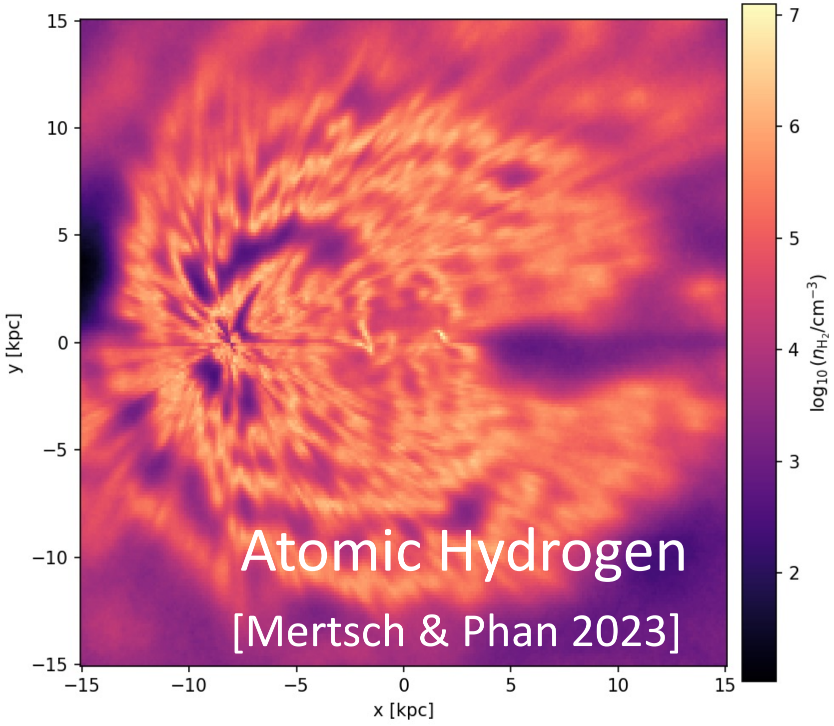

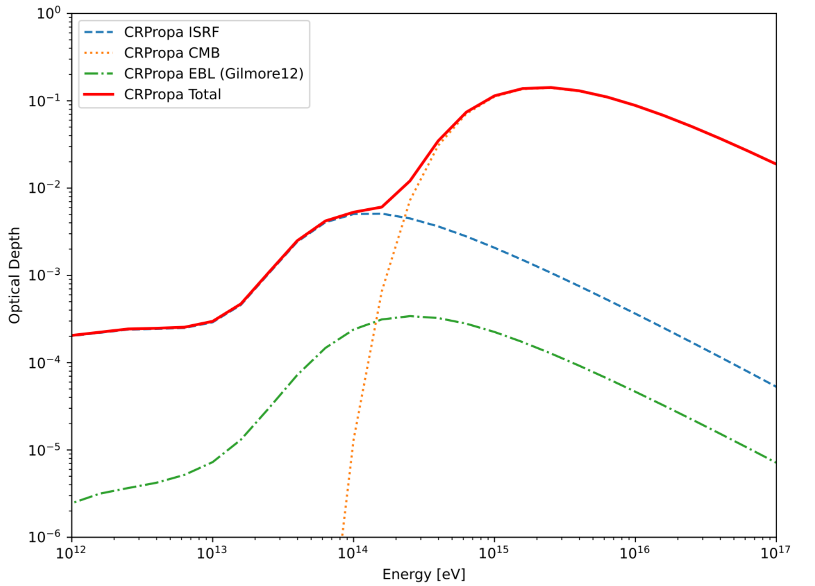

Absorption efficiency: CMB, EBL, ISRF

$$\phi_\nu(E_\nu,\Omega) = \frac{1}{4\pi}\int dE_{\rm p}\,\beta c\,\sigma_{pp}(E_{\rm p})\,\frac{dN_\nu}{dE_\nu}(E_\nu,E_{\rm p})\,X(\Omega,E_{\rm p})$$

$$X(\Omega,E_{\rm p}) = \int_0^\infty ds\,n_{\rm gas}(\mathbf{r})\,n_{\rm p}(E_{\rm p},\mathbf{r})$$

Anchor in CR data

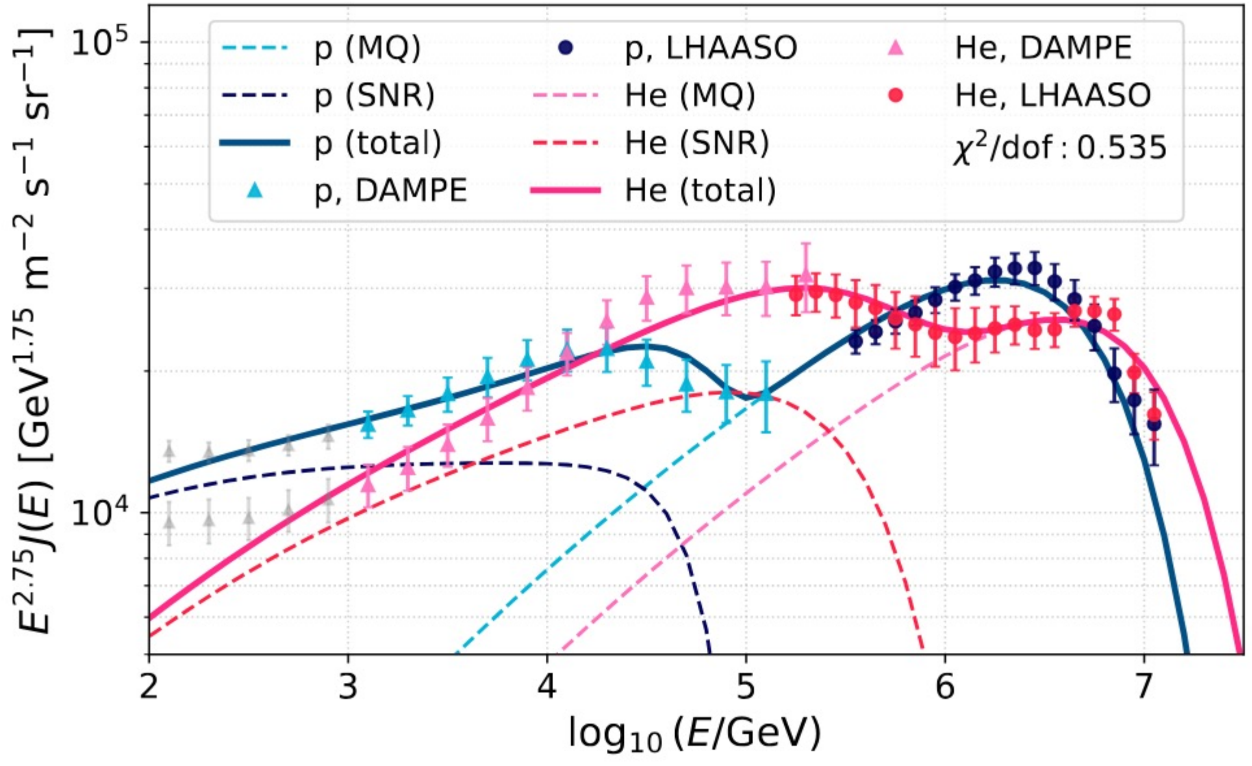

[Yu & Zhang, 2026, arXiv: 2608.22374]

Joint fit to proton and helium data observed by LHAASO and DAMPE

We adopt separate injection parameters for proton and helium [Aharonian & Zhang, ApJ, 2026], but keeps the normalization as free parameter

- Supernova $\mathcal{E}_{\rm cr} = \eta_{\rm cr,SN}\mathcal{E}_{\rm SN}$
- Microquasar $L_{\rm cr} = \eta_{\rm cr,MQ}L_{\rm Edd}$

CR acceleration efficiencies $\eta_{\rm CR}$ best-fit values with 1σ uncertainty bounds

Component	Parameter	Best-Fit Value $\pm 1\sigma$
Microquasars	$\eta_{p,\rm MQ}$	0.10 ± 0.009
	$\eta_{\rm He,\ MQ}$	0.02 ± 0.0004
SNRs	$\eta_{p,\rm SN}$	0.11 ± 0.035
	$\eta_{\rm He,\ SN}$	0.04 ± 0.0017

Predicted Diffuse Neutrinos

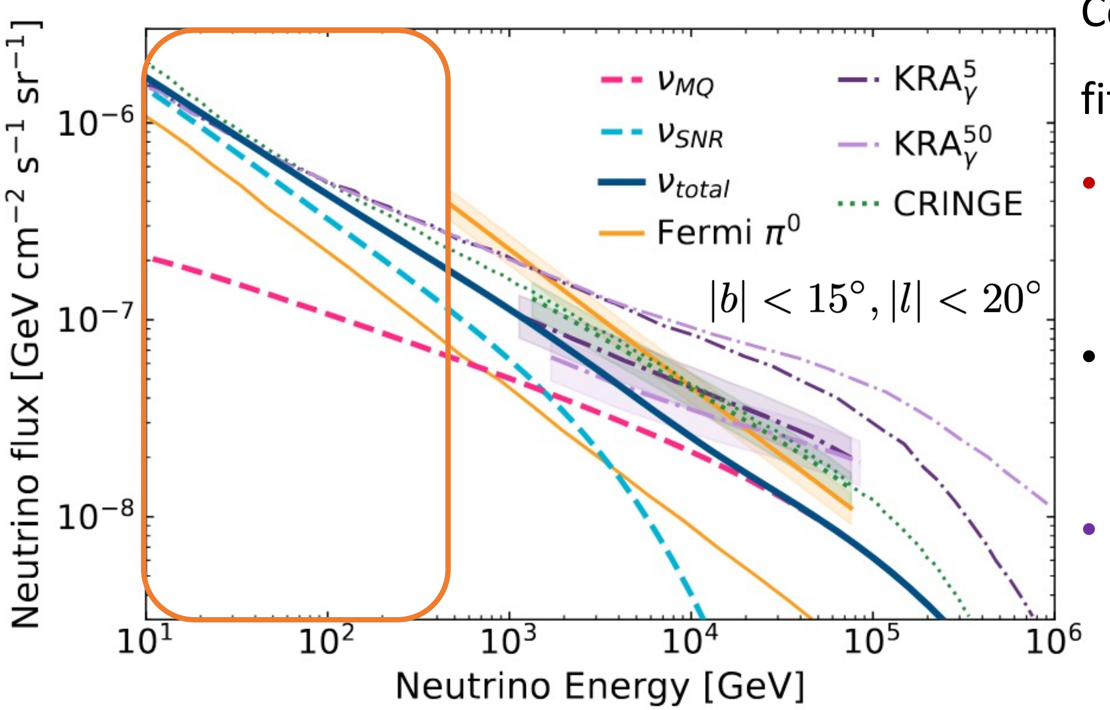

Potential room for contributions from additional/alternative sources or acceleration/propagation physics

High-precision data points are essential for rigorous model comparison and constraint

[Yu & Zhang, 2026, arXiv: 2608.22374]

Comparison between nominal template predictions and IceCube best fits reveals distinct energy regimes

- Sub-TeV regime: agreement across models
  - SNR dominant and everyone fitted to <10 TeV CR data.
- Beyond 10 TeV: MQ-dominated spectral hardening diverge from CRINGE and KRA
- KRA:
  - rely on simple extrapolations without constraints from recent high-energy CR data
- CRINGE:
  - fitted to KASCADE data and utilize rigidity-dependent diffusion breaks instead of source-driven cutoffs
- Our steepening is physically driven by maximum energy cutoffs of MQ and SNR populations

Predicted Diffuse Gamma Rays

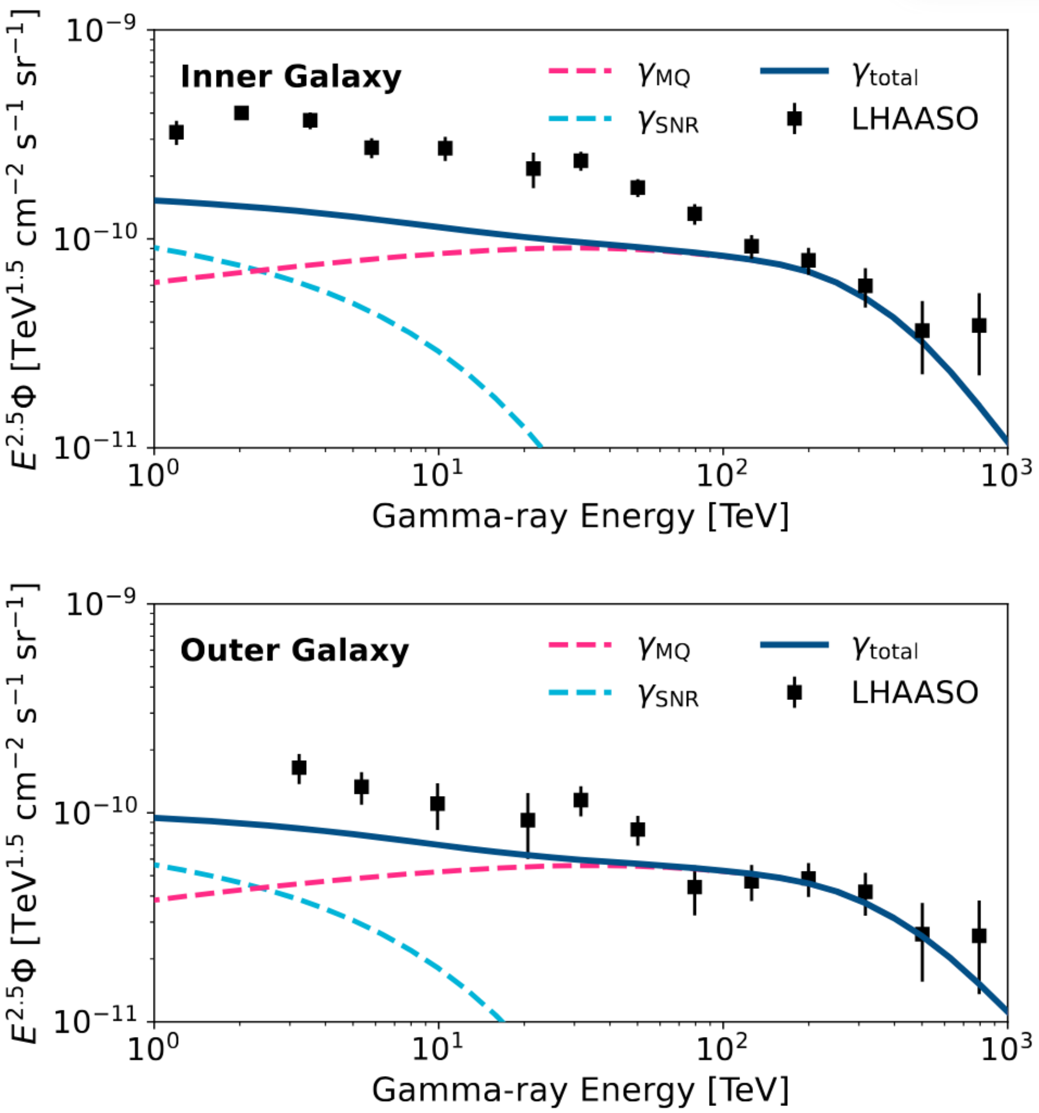

[Yu & Zhang, 2026, arXiv: 2608.22374]

Predicted diffuse gamma-ray fluxes in both inner and outer regions show consistency with LHAASO data

Below 100 TeV, a residual excess in the gamma-ray data suggests possible additional contributions:

- Unresolved, faint source populations
- Unmodeled leptonic process, such as inverse-Compton by high-energy electrons

Above 100 TeV, Inverse Compton emission is strongly suppressed by Klein-Nishina effects, transitioning the diffuse gamma-ray sky into a purely hadronic regime (better agreement)

Diffuse Sky Maps Imprinted by Microquasar and SNRs

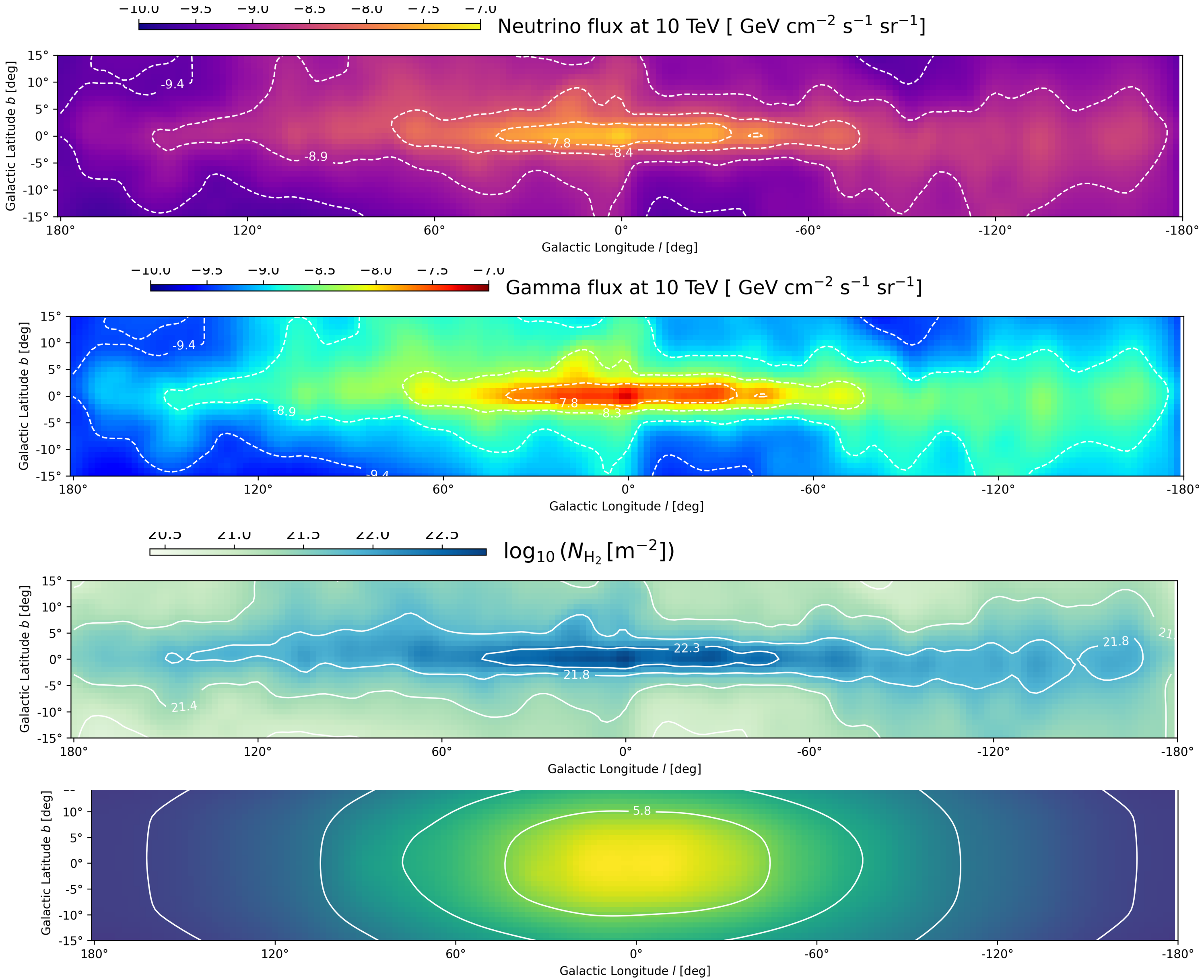

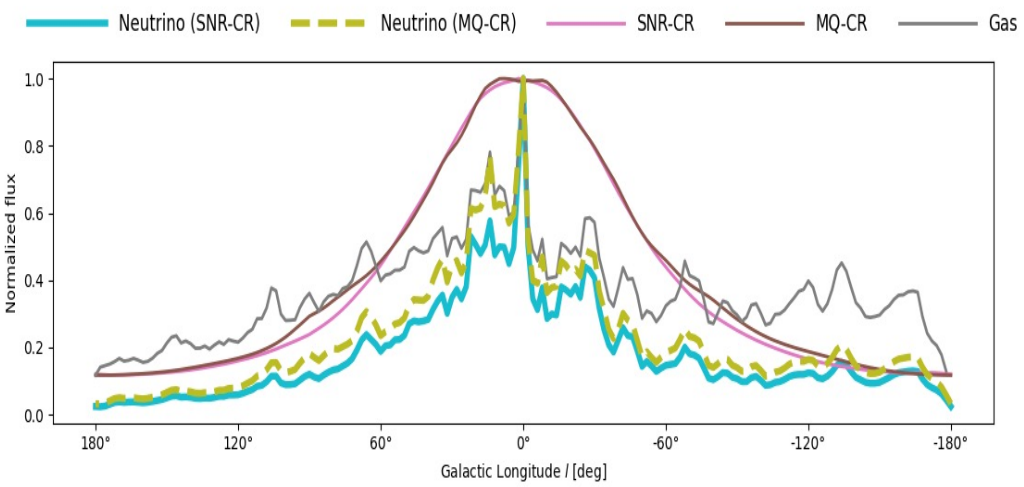

- CRs smoothly mirrors the large-scale radial distribution of the source population
- Secondary particle profiles closely track target gas morphology

Summary and discussion

The “knee” of the Galactic CR spectrum is one of the oldest puzzles in astroparticle physic, however, the situation has changed dramatically in recent years:

- Measurements of the proton and helium spectra around the knee have revealed an additional high-energy component

- UHE gamma-ray observations have revealed numerous Galactic sources emitting photons beyond 100 TeV

- Microquasars have recently emerged as particularly compelling candidates for the high-energy CR component

Summary and discussion

How about CR knee composition?

Composition of the CR knee

Our analysis shows that reaccelerating low-energy CRs (100 GV– 1 TV) yields a mean logarithmic mass roughly consistent with observations near the CR knee

Models assuming solar or enhanced solar compositions fail to reproduce the observed mass distribution.

	Z	A	Scenario 1: $f_{A,300\mathrm{GV}}$	Scenario 1: $f_{A,100\mathrm{GV}}$	Scenario 1: $f_{A,1\mathrm{TV}}$	Scenario 2: $f_\odot$	Scenario 3: $f_\odot^{\mathrm{enhance}}$
P	1	1	0.787	0.803	0.767	0.922	0.747
He	2	4	0.194	0.18	0.212	0.077	0.250
CNO	7	16	0.0145	0.013	0.0157	0.007	0.003
NeMgAlSi	12	28	0.00374	0.00352	0.004	0.001	0.0006
Fe	26	56	0.00121	0.00097	0.0014	0.00002	0.0001

TABLE II. Injected CR composition at the rigidity 300 GV, 100 GV, and 1 TV for different composition models. In addition, we also include solar composition $f_\odot$ and enhanced solar composition $f_\odot^{\mathrm{enhance}}$ by a factor of $(A/Z)^2$.

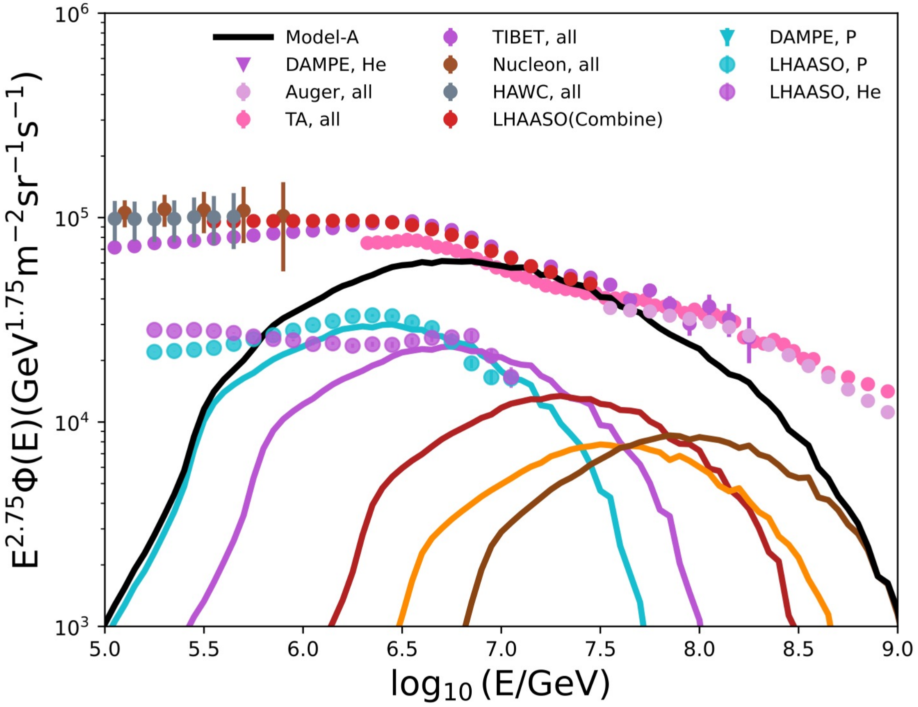

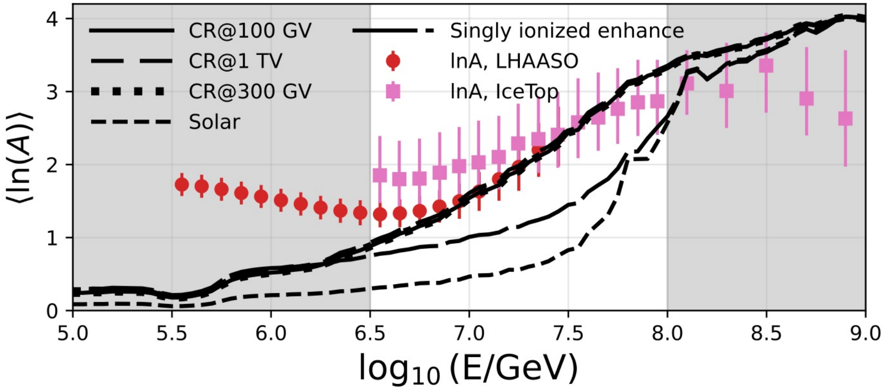

[BTZ, Kimura & Murase, 2025, PRD, arXiV: 2506.20193]

CR Reacceleration in microquasars and radio galaxies

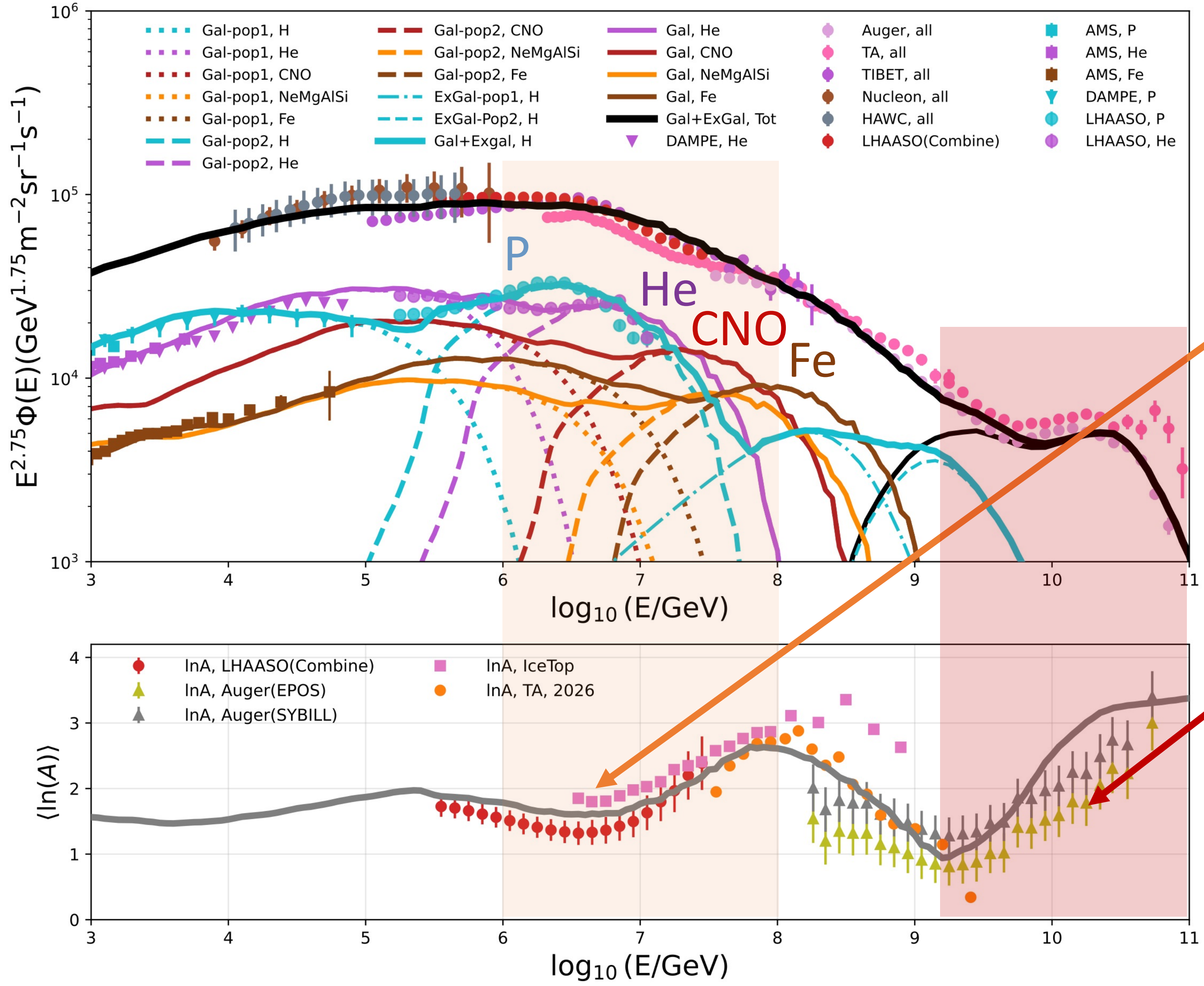

[BTZ, Kimura & Murase, 2025, PRD, arXiV: 2506.20193]

The reacceleration model works not only in the microquasars but also in the large-scale jet-cocoon system in radio galaxies

Gal pop2: CRs from microquasars (MQ)

Shear acceleration, Re-acceleration around 300 GV

[BTZ, Kimura & Murase, 2025, PRD, arXiV: 2506.20193]

ExGal pop2: UHECRs from radio galaxies (RG)?

Shear acceleration, Re-acceleration around 1 TV

[Kimura, Murase & BTZ, 2018, PRD, arXiV: 1705.05027]l

Summary and discussion

How about high-energy component?

Higher energy component ?

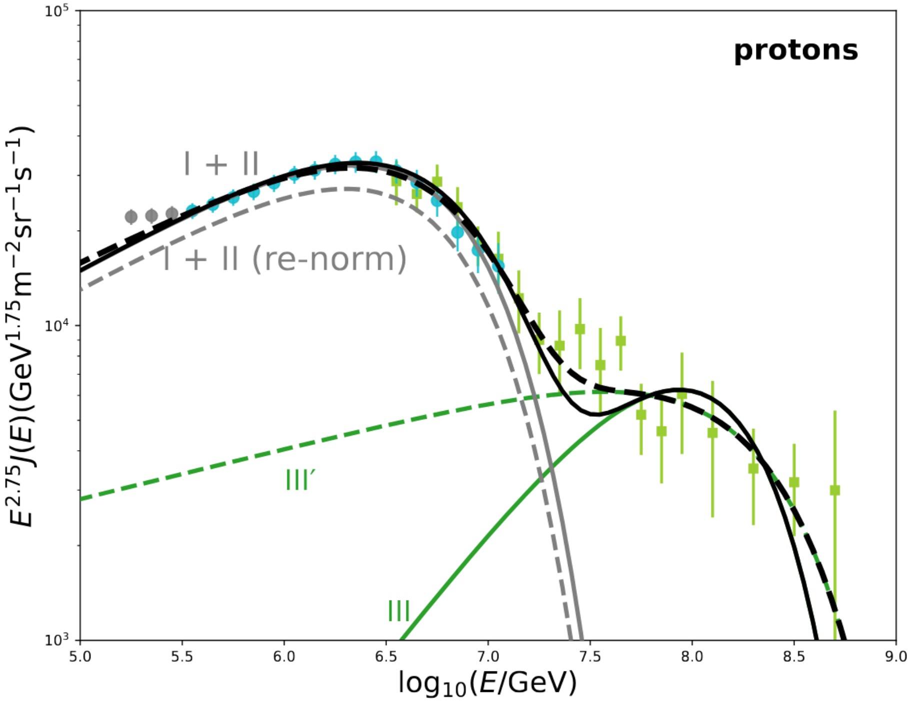

[Proton data from CALET, GRAPES-3 not shown for visibility]

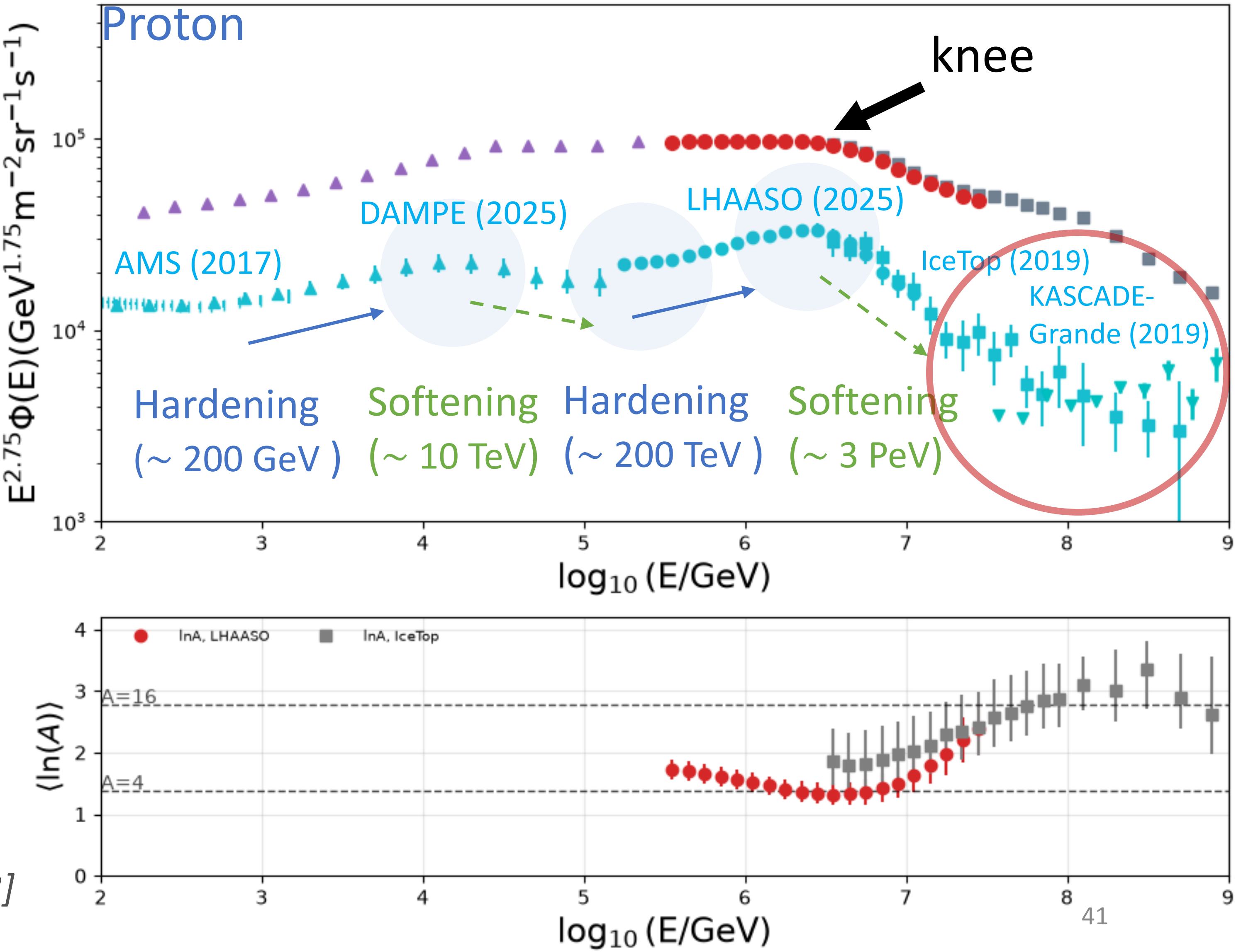

May be influenced by an additional contribution from a third CR proton component at energies of several tens to a few hundred PeV

[Aharonian and BTZ, 2026, ApJ, arXiv: 2062.08223]

Summary and discussion

Can we be more realistic?

This physically motivated framework (SNR + MQ) can be naturally extended to incorporate richer physical ingredients for Galactic diffuse CR, gamma-ray and neutrino:

- ✓ Galactic Magnetic Fields? Anisotropic and spatial dependent diffusion

  [E.g., Unger & Farrar 2023 (coherent field), Unger & Farrar 2026 (Random field)]
- ✓ Population variations? High-mass X-ray binary (HMXB) and low-mass x-ray binary (LMXB)
- ✓ Refined source acceleration models? (e.g., DSA, shear, …)
- Composition measurement (e.g., iron and CNO spectrum)
- 3D Gas models (For secondary gamma-rays and neutrinos)
- Active source contributions (For secondary gamma-rays and neutrinos)
- …

Backup

Effects of anisotropic diffusion

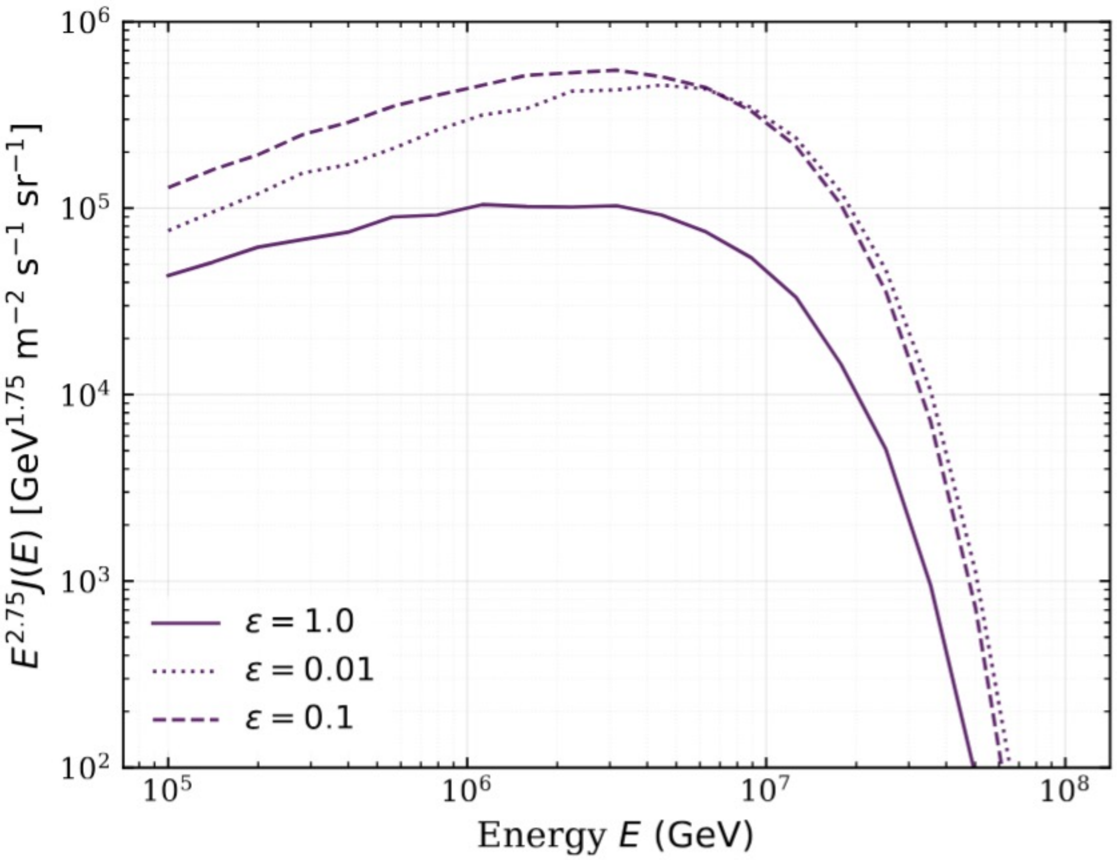

[Zhang & Yu, 2026, arXiv: 2602.08940]

Origin of CR knee: proton and helium spectrum

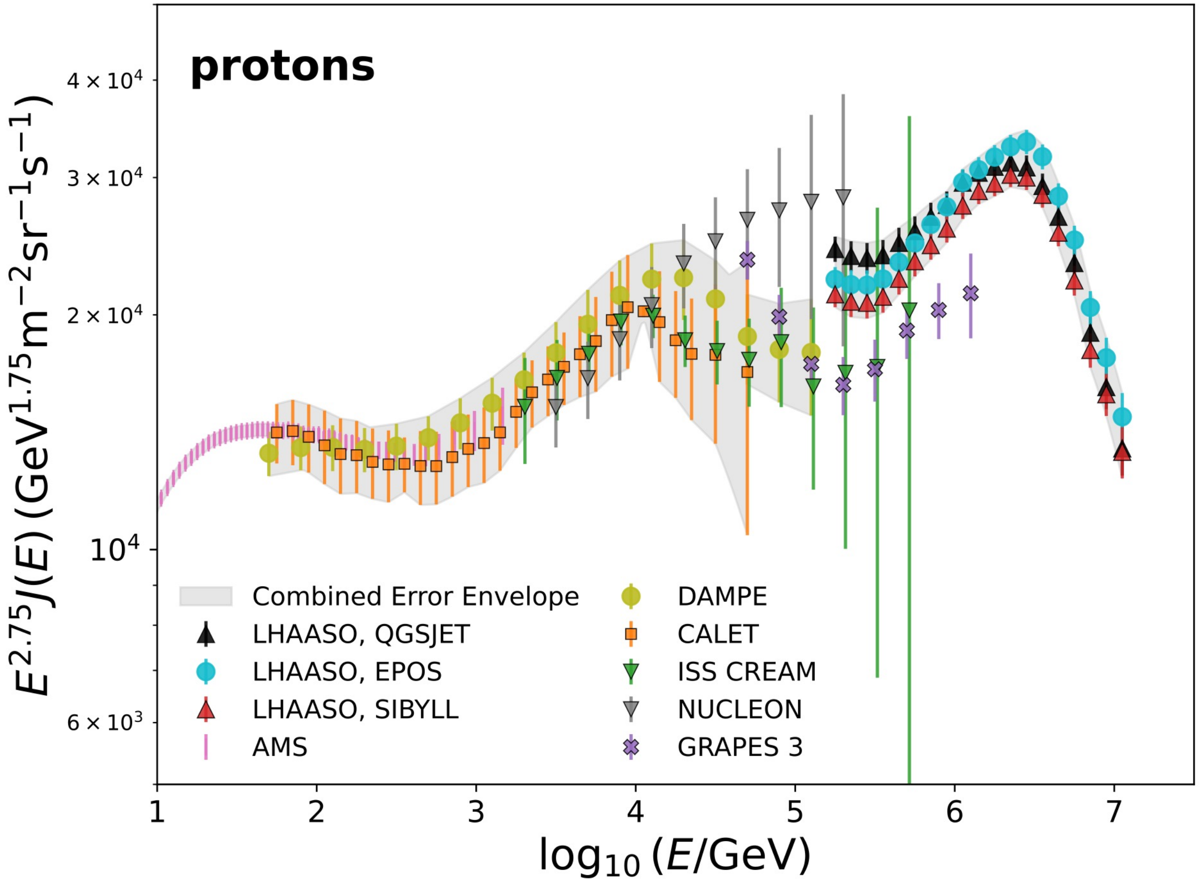

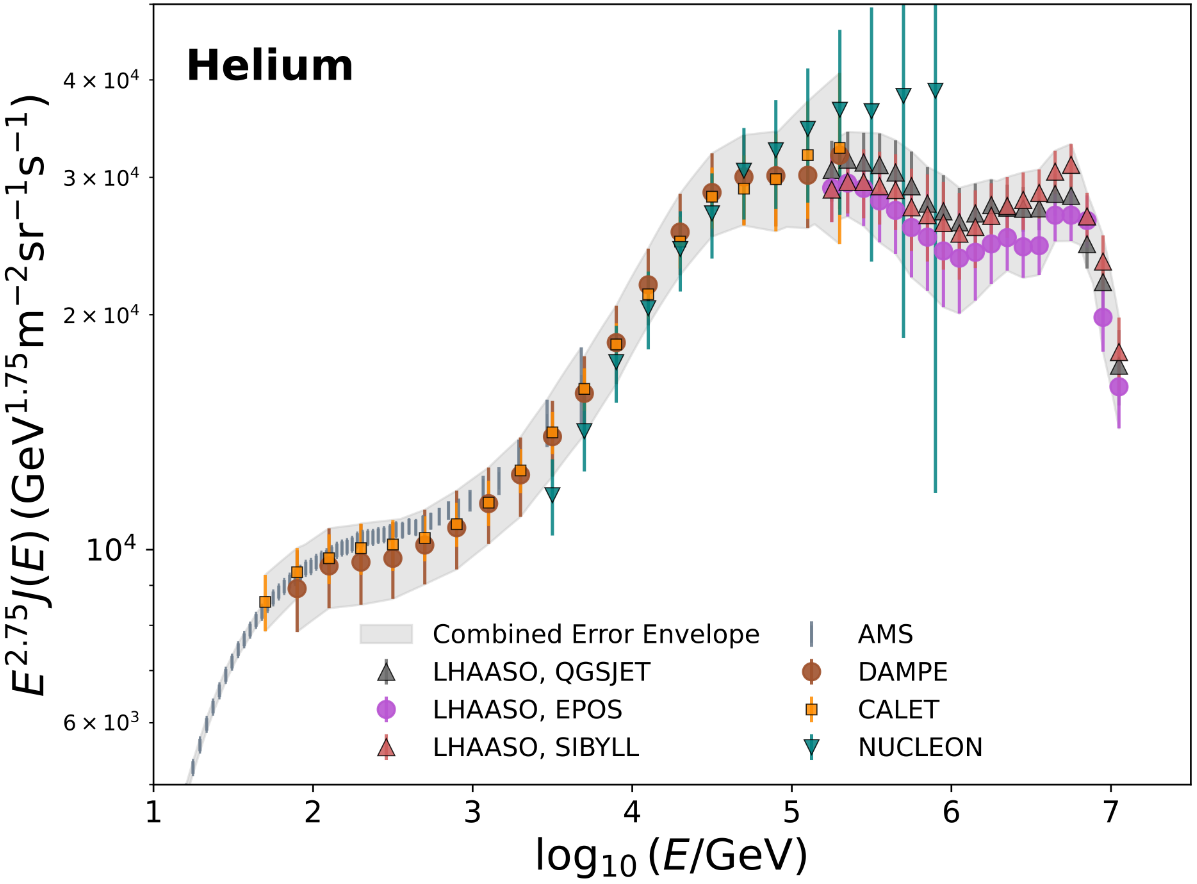

- LHAASO reported the high-purity proton spectrum, implicating the knee at the energy around 3 PeV is related to the change of the proton spectrum
- The observed hardening feature above several hundreds of TeV implicates the emergence of a new source component that has the maximum energy at least up to a few PeV

A Minimal Interpretation of the Galactic Cosmic Ray

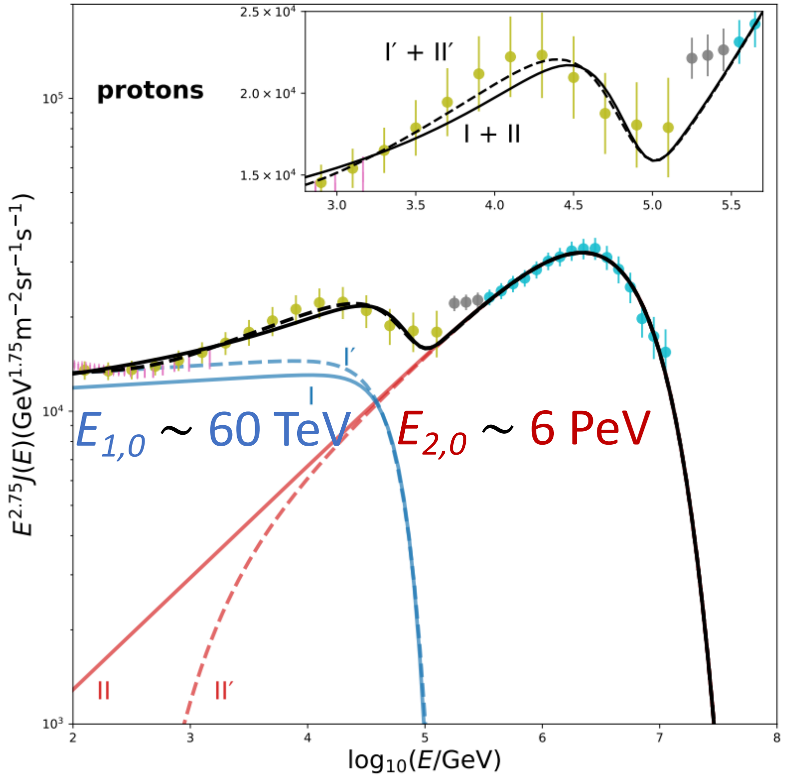

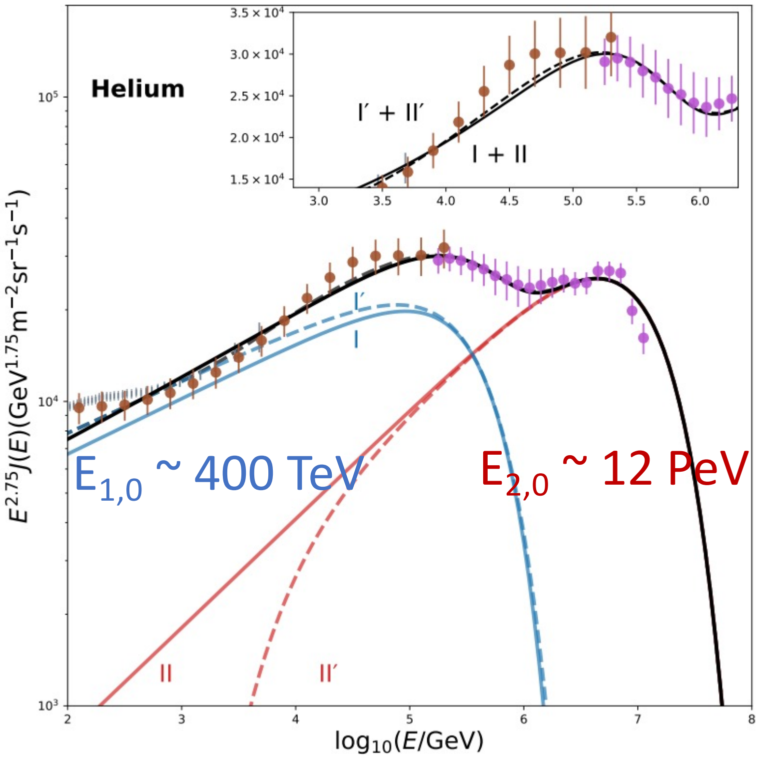

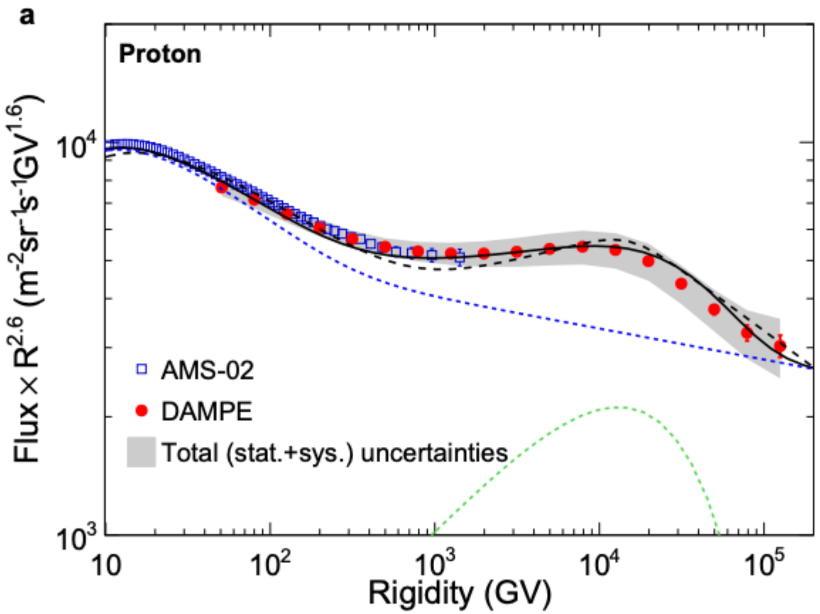

[DAMPE Coll. Nature, 2026]

[Aharonian and BTZ, 2026, ApJ, arXiv: 2062.08223]

TeV bump: Outcome of two source populations !!! Or a nearby source ?

Example: energy spectrum from shear acceleration

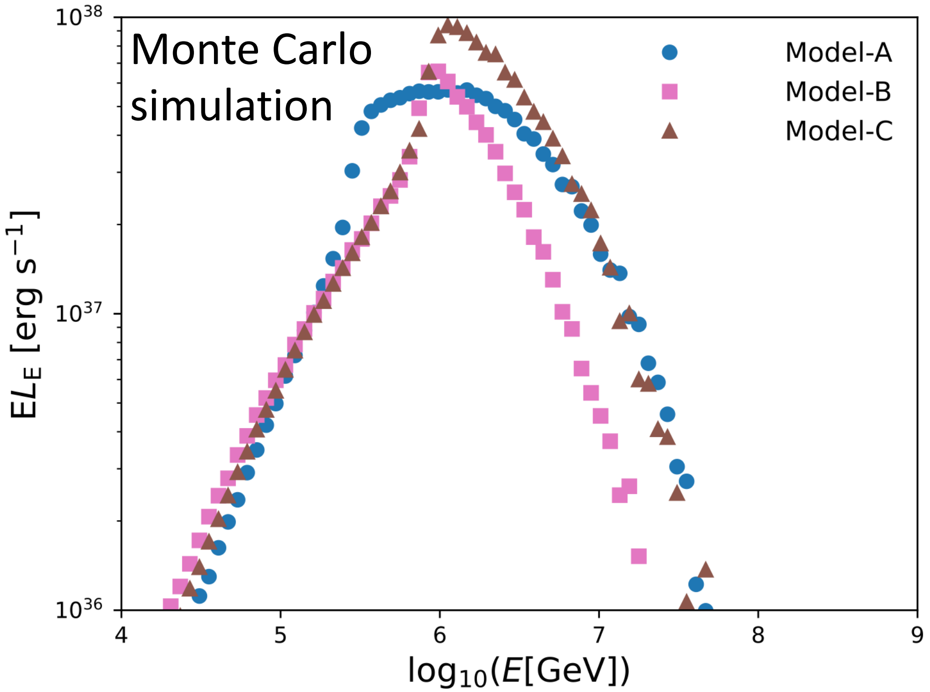

Model	$r_{\rm jet}$ [pc]	$B_{\rm jet}$ [μG]	$\beta_{\rm jet}$	$r_{\rm coc}$ [pc]	$B_{\rm coc}$ [μG]	$l_{\rm coh}$ [pc]	$l_{\rm jet}$ [pc]
A (default)	4	50	0.2	60	20	1.8	100
B	3	50	0.3	60	10	1.8	100
C	3	100	0.4	60	30	12	100

The escaping CR proton spectrum shows a hard component below the peak energy and a gradual cutoff above it

BTZ, Kimura & Murase, 2025, PRD, arXiV: 2506.20193

Balancing the acceleration and effective confinement timescales, the peak energy in the energy spectrum of escaping CR protons can be estimated to be:

$$t_{\rm conf} = \zeta_c R_{\rm jet}/c \sim t_{\rm acc} = \zeta_a \lambda_{\rm coc}/c\Gamma_{\rm jet}^2\beta_{\rm jet}^2$$

$$E_{\rm max} = \zeta e B_{\rm coc} l_{\rm coh}^{1/2} r_{\rm jet}^{1/2} \Gamma_{\rm jet}\beta_{\rm jet} \simeq 4.3~{\rm PeV} \left(\frac{B_{\rm coc}}{10\mu{\rm G}}\right)\left(\frac{l_{\rm coh}}{1.8~{\rm pc}}\right)^{1/2}\left(\frac{r_{\rm jet}}{3{\rm pc}}\right)^{1/2}\left(\frac{\beta_{\rm jet}}{0.3}\right)\zeta$$

Low-energy behavior below 100 GeV

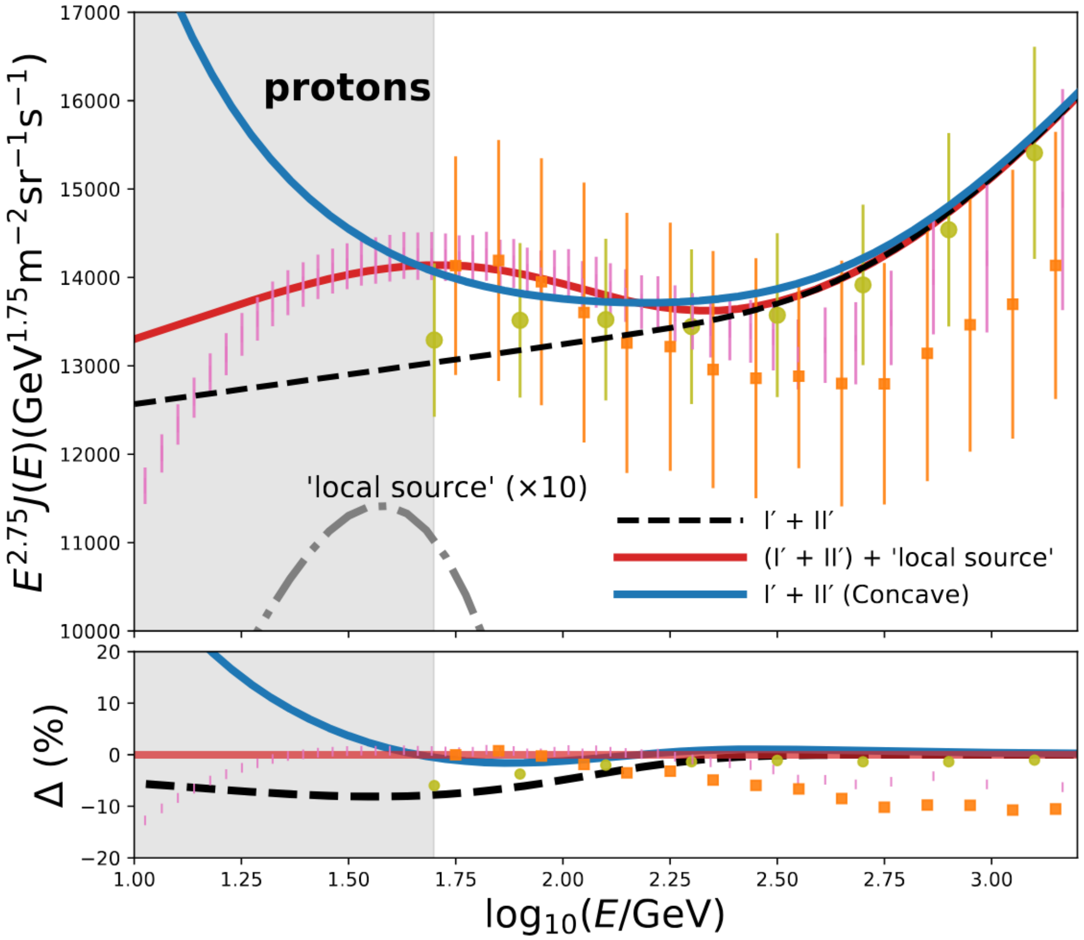

[Aharonian and BTZ, 2026, ApJ, arXiv: 2062.08223]

- A gradual low-energy steepening could arise from an additional nearby source contribution, reflect the contribution of local-source populations?
- Teflect the expected concavity of spectra produced within nonlinear DSA models

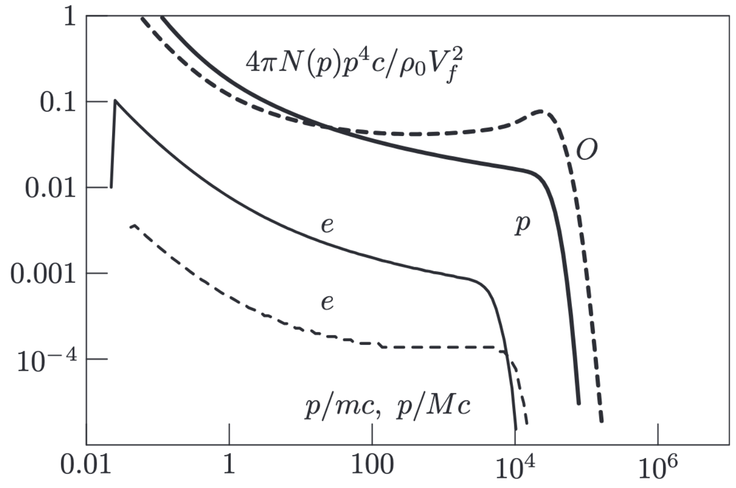

[V. Ptuskin et al. 2013; Zirakashvili et. al. 2014]

CRs from supernova and microquasar

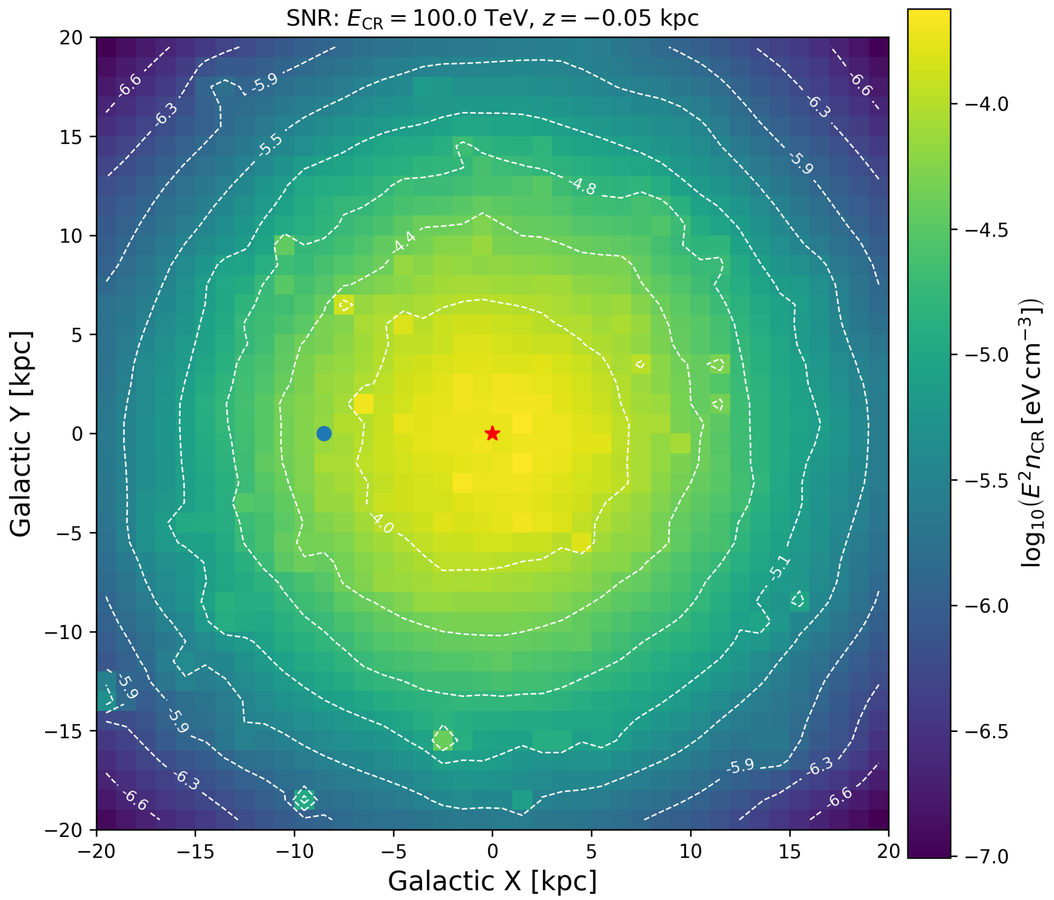

Illustration of steady-state CR density distribution of SNR at z=-0.05 kpc

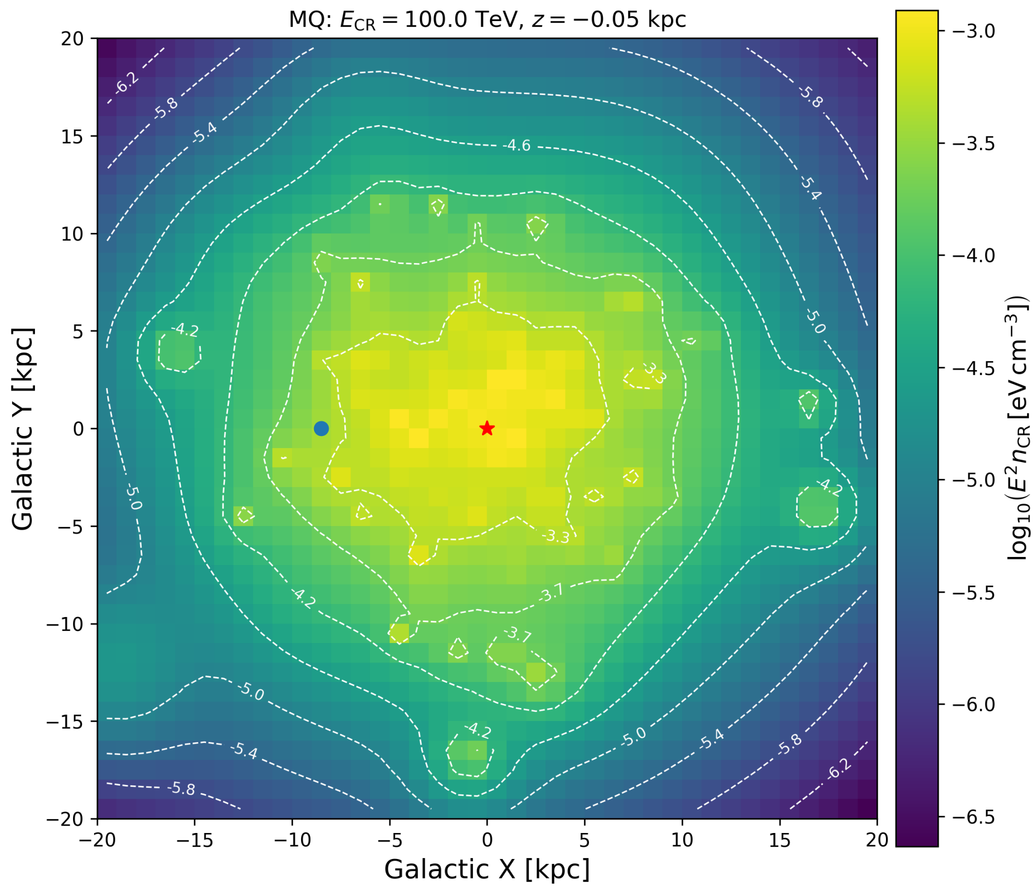

Illustration of steady-state CR density distribution of Microquasar at z=-0.05 kpc

Hadronic origin of the broadband gamma-ray spectrum

Power law with exponential cutoff

$$\mathrm{d}N/\mathrm{d}E = AE^{-s_{\rm cr}}\exp(-E/E_{\rm max})$$

- Energy budget: $W_p \approx 7.9^{+2.7}_{-2.4} \times 10^{49}(n_{\rm gas}/100\,{\rm cm}^{-3})^{-1}$ erg
- Spectral index: $s_{\rm cr} = 2.4$
- Max proton energy: $E_{p,\rm max} \approx 5.1^{+12.7}_{-2.8}$ PeV

The required proton injection rate:

$$Q_p \approx W_p/t_{\rm age} \simeq 2.5\times10^{37}\,(n_{\rm gas}/100\,{\rm cm}^{-3})^{-1}\,{\rm erg\ s^{-1}}$$

Jet with an average kinetic luminosity: $\bar{L}_{\rm jet} \sim 10^{39}\ {\rm erg\ s^{-1}}$

Age: $t_{\rm age} = 0.1\,{\rm Myr}$

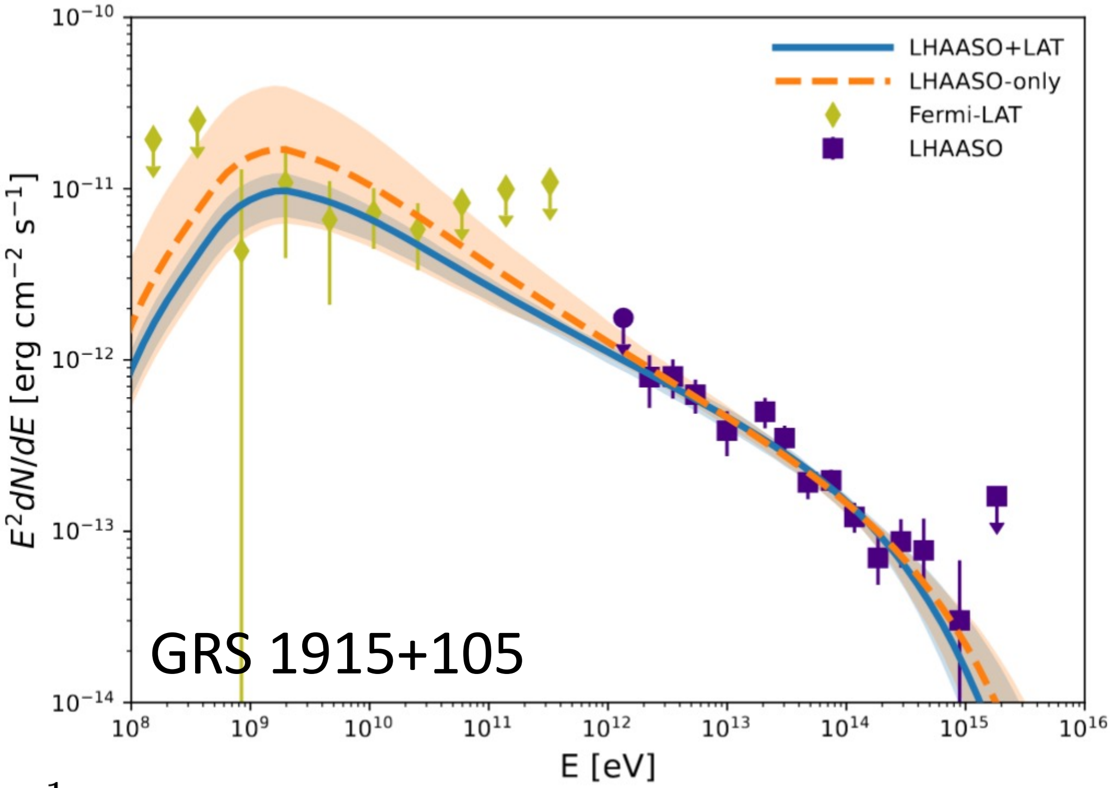

[LHAASO Collab., 2026, submitted]

Conclusion: The dense environment favors hadronic process, and supported by LHAASO observations; The accelerated CRs have hard spectrum with $s_{\rm cr,acc} \sim 2$

Maximum acceleration energy of CRs from microquasar

With the luminosity requirement obtained from the Hillas condition, the maximum possible energy of the accelerated CRs is estimated to be

$$E_{A,\max} \approx 3 \times 10^{16}\ \mathrm{eV}\ Z\epsilon_B^{1/2} \left(\frac{L_j}{10^{39}\ \mathrm{erg/s}} \right)^{1/2} \left(\frac{\beta}{0.3} \right)^{1/2}$$

- Z: Nuclear charge
- ϵ_B: Energy fraction carried by the magnetic field
- L_j: Jet kinetic energy
- β: Characteristic velocity normalized by the speed of light

The black-hole Eddington luminosity $L_{\mathrm{Edd}} \sim 10^{39}$ (M / 10 M_{sun}) erg s^{-1}

In our Galaxy, there are likely a few dozens of BH X-ray binaries with an X-ray luminosity of $L_X \gtrsim 10^{38}$ erg s^{-1}, each exhibiting sufficient luminosity, $L_j \sim 10^{39}$ erg s^{-1}

Energy spectrum from Shear acceleration

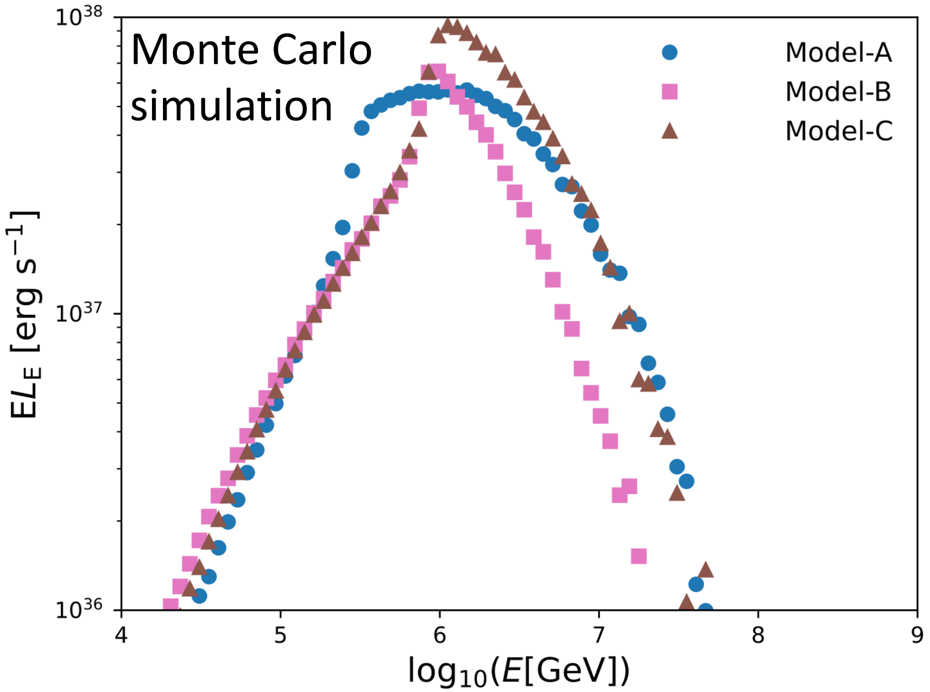

[Zhang, Kimura & Murase, 2026, PRD]

Model	$r_{\rm jet}$ [pc]	$B_{\rm jet}$ [μG]	$\beta_{\rm jet}$	$r_{\rm coc}$ [pc]	$B_{\rm coc}$ [μG]	$l_{\rm coh}$ [pc]	$l_{\rm jet}$ [pc]
A (default)	4	50	0.2	60	20	1.8	100
B	3	50	0.3	60	10	1.8	100
C	3	100	0.4	60	30	12	100

The escaping CR proton spectrum shows a hard component below the peak energy and a gradual cutoff above it

Balancing the acceleration and effective confinement timescales, the peak energy in the energy spectrum of escaping CR protons can be estimated to be:

$$t_{\rm conf} = \zeta_c R_{\rm jet}/c \;\sim\; t_{\rm acc} = \zeta_a \lambda_{\rm coc}/c\Gamma_{\rm jet}^2\beta_{\rm jet}^2$$

$$E_{\rm max} = \zeta e B_{\rm coc} l_{\rm coh}^{1/2} r_{\rm jet}^{1/2} \Gamma_{\rm jet}\beta_{\rm jet} \simeq 4.3\ {\rm PeV} \left(\frac{B_{\rm coc}}{10\mu{\rm G}}\right)\left(\frac{l_{\rm coh}}{1.8\ {\rm pc}}\right)^{1/2}\left(\frac{r_{\rm jet}}{3{\rm pc}}\right)^{1/2}\left(\frac{\beta_{\rm jet}}{0.3}\right)\zeta$$

Discrete shear acceleration and CR injection

CRs will undergo a discrete shear acceleration, when the CR mean free path is longer than the width of the sheath layer: $\lambda \gtrsim r_{\rm sl}$

- The mean free path of CRs: $\lambda \sim l_{\rm coh}(E/E_{\rm coh})^{\delta}$
- For Kolmogorov turbulence: $\delta = 1/3$
- The coherence length inside the cocoon: $l_{\rm coh} \sim 0.03 r_{\rm coc} \sim 1.8\ {\rm pc}$
- The typical energy: $E_{\rm coh} = ZeB_{\rm coc}l_{\rm coh} \sim 17Z(B_{\rm coc}/10\ \mu{\rm G})(l_{\rm coh}/1.8\ {\rm pc})\ {\rm PeV}$
- The width of the sheath layer: $r_{\rm sl} \sim f_{\rm sl} r_{\rm jet} \sim 0.06(f_{\rm sl}/0.02)\ {\rm pc}$

The injection energy is given by $\lambda \sim r_{\rm sl}$

$$E_{\rm inj} \approx E_{\rm coh}\left(\frac{r_{\rm sl}}{l_{\rm coh}}\right)^3 \sim 0.6\left(\frac{B_{\rm coc}}{10\mu{\rm G}}\right)\left(\frac{r_{\rm sl}}{0.06\ {\rm pc}}\right)^3\left(\frac{l_{\rm coh}}{1.8{\rm pc}}\right)^{-2}\ {\rm TeV}$$

CRs with energies above several hundreds of GeV can undergo a discrete shear acceleration mechanism

Basic setup

[Zhang, Kimura & Murase, 2026, PRD]

We employ a publicly available version of the DRAGON code to propagate CRs

- The maximum value of Galactocentric radius is 10 kpc and halo size is 4 kpc
- The spatial distribution of the diffusion coefficient (Constrained from boron to carbon ratio)

$$D = 23.8 \times 10^{28} (\mathcal{R}/250\ \mathrm{GV})^{\delta} \mathrm{cm}^2\ \mathrm{s}^{-1} \quad \mathcal{R} \geqslant 250\ \mathrm{GV}, \delta = 1/3$$

The spatial distribution of microquasars is unknown, but high-Eddington ratio microquasars, including SS 433 or Sgr V4641, likely follow the distribution of massive stars

- Assume similar spatial distribution with Galactic SNRs (Ferriere2001) and adopt continuous source distribution

See also Galactic X-ray binary radial distribution
[Yue, J. Zhang, …, Guo & Hu, ApJ, 2026]

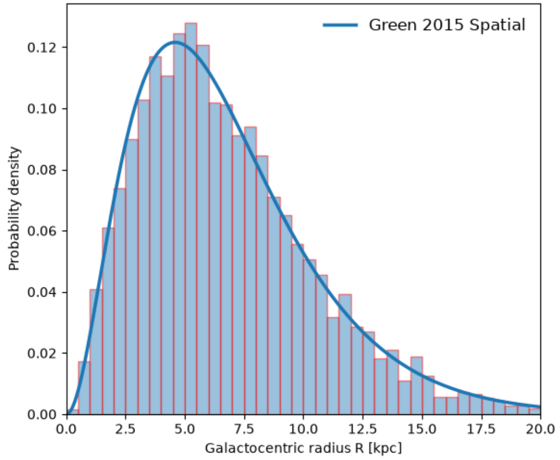

Observed CR spectrum and composition on Earth

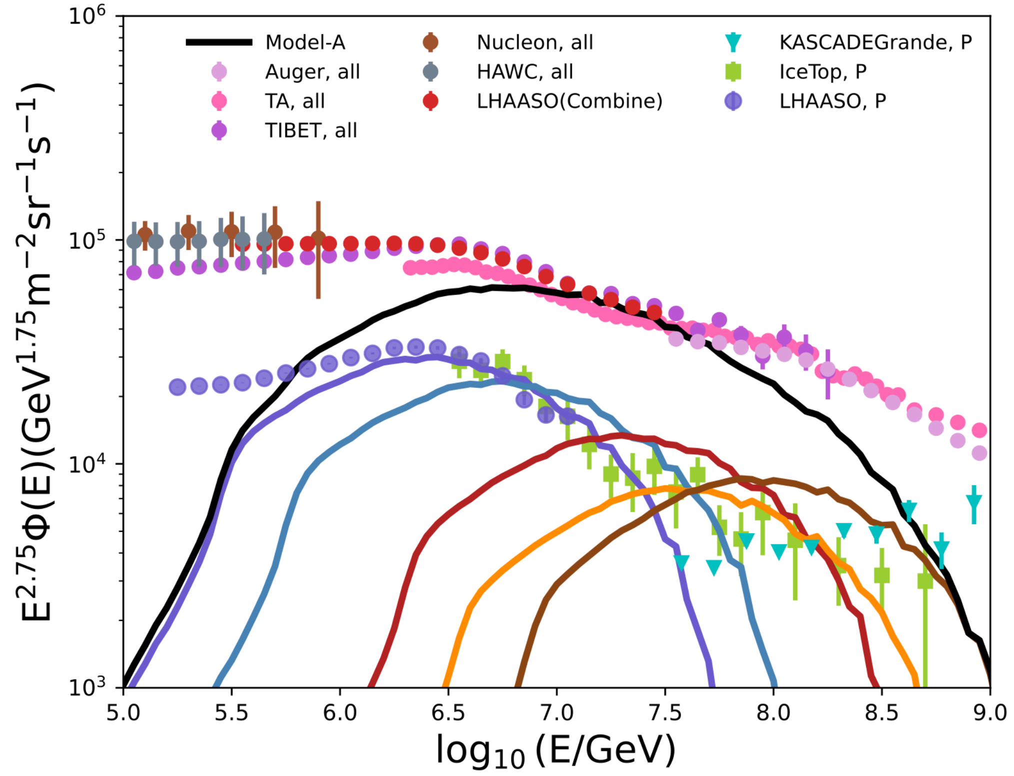

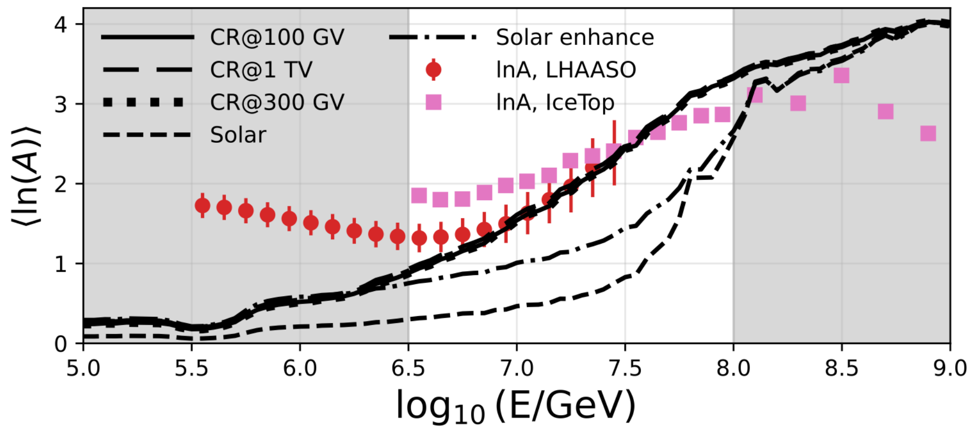

The energy injection rate density of CRs:

$$Q_{\rm cr,tot} \sim 1.3 \times 10^{42} \ {\rm erg\ kpc^{-3}\ yr^{-1}}$$

The energy injection rate integrated over the Galactic volume:

$$L_{\rm cr,tot} = Q_{\rm CR,tot} V_G \simeq 1.5 \times 10^{38} \ {\rm erg\ s^{-1}}$$

Consistent with the value required to explain CRs in the knee energy range if we have around 3-10 microquasars with extended jets in our Galaxy

E.g., SS 433 and V4641 Sgr with extended jet ~ 100 pc

Origin of the knee – Propagation effect?

- Cosmic ray propagation inside galaxy

e.g., *Syrovatsky (1971), Ptuskin (1992), Giacinti (2014,2015)*

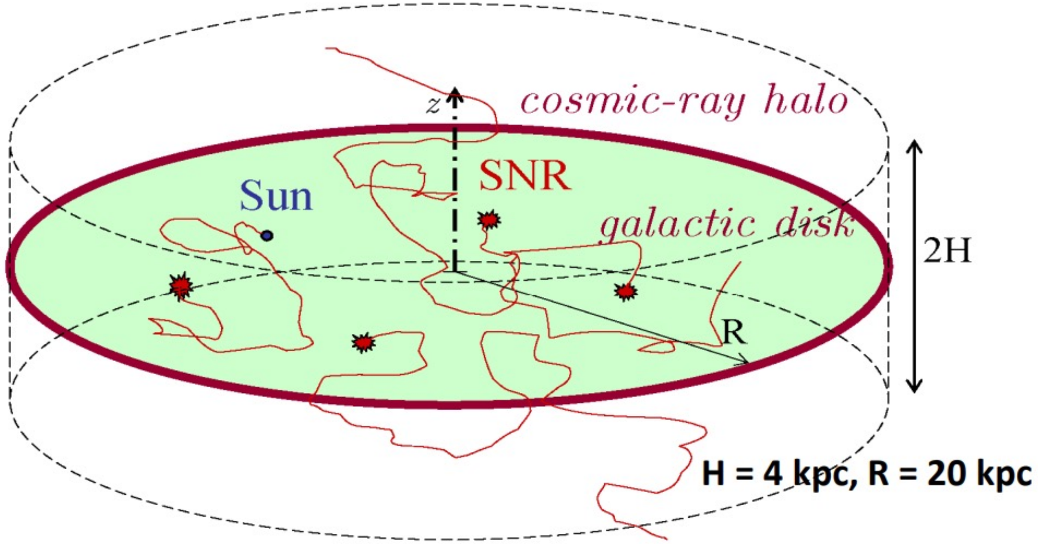

Constant diffusion coefficient

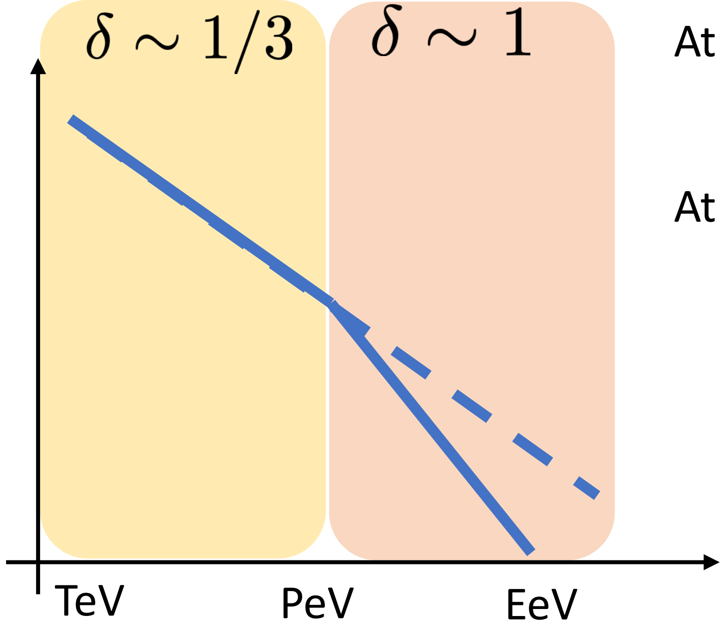

At Source:

$$\mathcal{R}^2 dN/d\mathcal{R} \propto \mathcal{R}^{2-s_{\rm sec}}$$

At Earth:

$$\mathcal{R}^2 \Phi_{\mathcal{R}} \propto (\mathcal{R}^2 dN/d\mathcal{R}) X_{\rm esc}$$
$$\propto \mathcal{R}^{2-s_{\rm esc}-\delta}$$

The grammage traversed by CRs during propagation $X_{\rm esc} \simeq \mathcal{R}^{-\delta}$